Geological features and origin of gold deposits occurring in the Baotou–Bayan Obo district, south-central Inner Mongolia, People's Republic of China

Feng-Jun Nie [a,*], Si-Hong Jiang [a], Xin-Xu Su [b], Xin-Liang Wang [b]

[a]Institute of Mineral Deposits, Chinese Academy of Geological Sciences, Baiwanzhuang Road 26, Beijing 100037, China
[b]Inner Mongolian Geological Survey, Hohhot 010020, Inner Mongolia Autonomous Region, China

Abstract

Located at western portion of northern margin of North China craton, the Baotou–Bayan Obo district is one of the most important Fe–REE–Nb and Au metallogenic provinces in China. Presently, about 52 gold deposits and prospects have been discovered, explored and mined, among which Shibaqinhao, Laoyanghao, Houshihua, Saiyinwusu, Wulashan and Donghuofang are the most important ones. All these gold occurrences can be subdivided into three groups (or types) according to its host rocks: (1) hosted by Archean high-grade metamorphic rocks; (2) hosted by Proterozoic sedimentary rocks; (3) hosted by or related to Hercynian alkaline intrusive rocks. The first group contains the Shibaqinhao, Laoyanghao and Houshihua gold deposits. Gold mineralization at these three deposits occurs within Archean amphibolite, gneiss and granulite as gold-bearing quartz veins and veinlet groups containing native gold, electrum, pyrite and chalcopyrite. The Saiyinwusu deposit belongs to the second group, and occurs within Proterozoic sandstone, quartzite and carbonaceous slate as quartz veins and replacement bodies along the fracture zones. Pyrite, marcasite, arsenopyrite, native gold and electrum are identified. The third group includes the Wulashan, Donghuofang and Luchang deposits. Gold mineralization at these three deposits occurs predominantly within the Hercynian alkaline syenite or melagabbro stocks and dyke swarms or along their contacts with Archean metamorphic wall rocks as K-feldspar–quartz veins, dissemination and veinlets. Pyrite, galena, chalcopyrite, native gold and calaverite are major metallic minerals. $\delta^{34}S$ value of sulfides (pyrite, galena and pyrrhotite) separates from groups 1 and 2 varies from $-4.01‰$ to $-0.10‰$ and $-3.01‰$ to $2.32‰$, respectively. $\delta^{34}S$ values of Archean and Proterozoic metamorphic wall rocks for groups 1 and 2 deposits range from $-20.2‰$ to $-17.0‰$ and $-15.8‰$ to $-16.2‰$, respectively. The values are much lower than their hosted gold deposits. All these pyrite separates from Hercynian alkaline intrusions associated with the gold deposits show positive $\delta^{34}S$ values of $1.3‰$ to $4.8‰$, which is higher than those Precambrian metamorphic wall rocks and their hosted gold deposits. $\delta^{34}S$ values of the sulfides (pyrite and galena) from the Donghuofang and Wulashan deposits (group 3) increase systematically from veins ($-14.8‰$ to $-2.4‰$) to the Hercynian alkaline igneous wall rocks ($2.8‰$ to $4.8‰$). All of these deposits in groups 1, 2 and 3 show relatively radiogenic lead isotopic compositions compared to mantle or lower crust curves. Most lead isotope data of sulfides from the gold ores plot between the Hercynian alkaline intrusions and Precambrian metamorphic wall rocks. Data are interpreted as indicative of a mixing of lead from mantle-derived alkaline magma with lead from Precambrian metamorphic wall rocks. Isotopic age data, geological and geochemical evidence suggest that the ore fluids for the groups 1 and 2 deposits were generated during the

---

* Corresponding author. Tel.: +86-10-68327181; fax: +86-10-68327263.
   E-mail address: nfjj@mx.cei.gov.cn (F.-J. Nie).

emplacement of the Hercynian alkaline syenite and mafic intrusions. The Hercynian alkaline magma may provide heat, volatiles and metals for these groups 1 and 2 deposits. Evolved metamorphic fluids produced by the devotalization, which circulated the wall rocks, were also progressively involved in the alkaline magmatic hydrothermal system, and may have dominate the ore fluids during late stage of ore-forming processes. Most of these gold deposits hosted by Archean high-grade metamorphic rocks occur at or near the intersections of the NE- and E–W-trending fracture systems. The ore fluid of the group 3 deposits may have resulted from the mixing of Hercynian alkaline magmatic fluids and evolved meteoric waters. The deposits are believed to be products of Hercynian alkaline igneous processes along deep-seated fault zones within Archean terrain. © 2002 Elsevier Science B.V. All rights reserved.

1. Introduction

The Baotou–Bayan Obo district, located about 155 km west of Hohhot, the capital city of Inner Mongolia (Fig. 1), has been known as the most important REE and Nb metallogenic province in the world since the discovery of the supergiant Bayan Obo Nb–REE–Fe deposit in 1927 (Institute of Geochemistry, Chinese Academy of Sciences, 1988; Bai et al., 1996). The unique geological and geochemical features of the district have attracted abundant attention from both Chinese and international geologists (Drew et al., 1990; Chao et al., 1992; Yuan et al., 1992; Conrad and McKee, 1992; Gordon, 1993; Nie and Bjørlykke, 1994; Bai et al., 1996; Zhang et al., 1999). Systematic mineral exploration for gold, iron, rare earth elements and base metals started in the 1950s up to the present; over 52 gold deposits and prospects have been identified, some of which have been explored and mined. All these gold occurrences can be subdivided into three groups according to their host rocks: (1) those hosted by Archean high-grade metamorphic rocks. The representative deposits include Shibaqinhao, Laoyanghao and Houshihua; (2) those hosted by Proterozoic sedimentary rocks. Saiyinwusu is the best example, and (3) those hosted by or related to Hercynian alkaline intrusive rocks. Typical deposits include Wulashan and Donghuofang deposits.

Among these gold occurrences, the Wulashan deposit is the largest one, and exhibits intriguing and instructive similarities to the alkaline-type gold deposits (Mutschler et al., 1985; Bonham, 1988; Richards and Kerrich, 1993; Richards, 1995; Nie and Wu, 1998; Nie, 1998). Although most of gold deposits and prospects occur within the Precambrian metamorphic rocks, there has been renewed explora-

tion and mining activities focused on the Hercynian alkaline intrusions since the discovery of the Wulashan deposit (Nie and Bjørlykke, 1994). As a result, the Donghuofang deposit occurring within a Hercynian alkaline syenite stock has been located. Data from the newly discovered Wulashan and Donghuofang deposits indicate that a substantial gold resource exists in the district. The Wulashan, Saiyinwusu and Shibaqinhao deposits have been operating since 1987, 1988 and 1991, respectively. The mine construction at Laoyanghao and Donghuofang has commenced. The aggregate gold production to data from these gold mines is about 35 t Au (Zhang et al., 1999).

Some geologic and geochemical data on individual gold deposits of the district have been published both in internal and national journals of geological sciences (Guo and Wu, 1989; Lang, 1990; Zhang, 1991; Guan, 1993; Chen et al., 1996; Jia et al., 1999). The deposit geology, lead and sulfur isotopic features of the Wulashan deposit were described by Gan et al. (1994) and Nie and Bjørlykke (1994). Emplacement of the Hercynian alkaline intrusions played an important role during the formation of the Wulashan deposit (Nie and Bjørlykke, 1994; Chen et al., 1996). In a recent paper on regional metallogenesis of the Baotou–Bayan Obo district, Zhang et al. (1999) also pointed out that gold mineralization is genetically associated with late Paleozoic magmatism and structural activity.

The regional geological setting and metallogenesis of the Baotou–Bayan Obo district have been discussed; however, the detailed ore-forming processes of these gold deposits occurring in the district, especially the genetic relation between the gold mineralization and tectono-magmatic activity, have not been reported. This paper describes the basic geologic and

geochemical features of the major gold deposits of the Baotou–Bayan Obo district. New sulfur and lead isotopic data are also reported, with the aim of constraining the possible sources of gold and the ore-forming processes. Some considerations are presented concerning the genetic relations between gold mineralization, magmatism and regional tectonic evolution.

2. Geological settings

The major stratigraphic units, structures and intrusive bodies in the Baotou–Bayan Obo district are shown in Fig. 1. The district is divided into three parts by the Chuanjing-Bulutai deep-seated fault and the Shetai–Guyang–Wuchuan faulted shear zone. These parts are (1) Archean basement to the south;
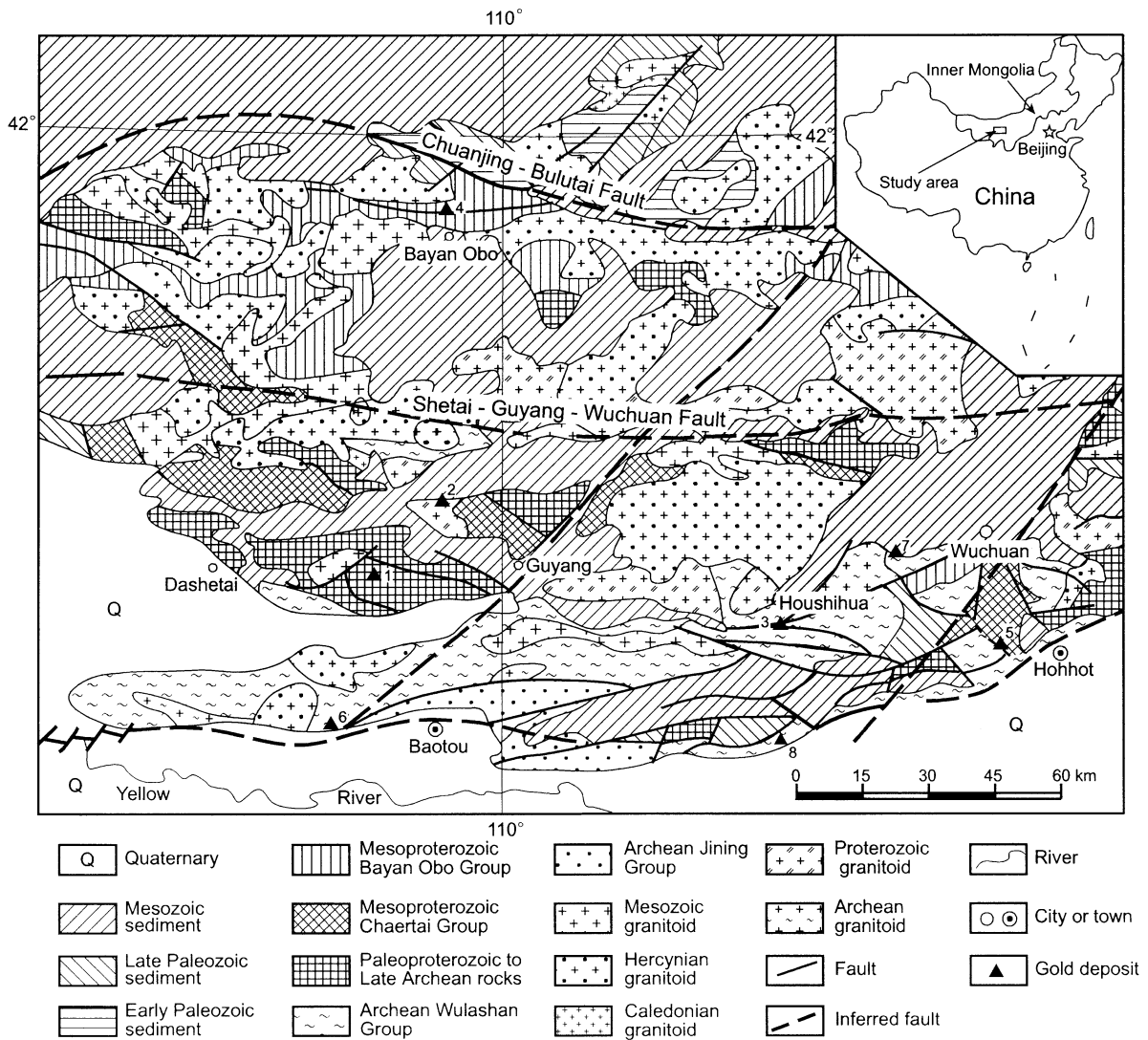

Fig. 1. Simplified geological map showing the location of major gold deposits in the Baotou–Bayan Obo district and its neighboring area. (1) Shibaqinhao gold deposit; (2) Laoyanghao gold deposit; (3) Houshihua gold deposit; (4) Saiyinwusu gold deposit; (5) Motianling gold deposit; (6) Wulashan gold deposit; (7) Donghuofang gold deposit; (8) Luchang gold deposit.

(2) Proterozoic metamorphosed volcanic and sedimentary sequences in the center; and (3) Proterozoic to Paleozoic transition zone to the north. It is noted that the district has been influenced by repeated distinct tectono-magmatic activities (Geological Institute of Inner Mongolia, 1988; Bureau of Geology and Mineral Resources of Inner Mongolia, 1991; Davis et al., 1998; Miller et al., 1998; Zhang et al., 1999). Most of these gold deposits occur within the Archean to Proterozoic metamorphic rocks in southern and central parts of the district, but all of them show an intimate spatial relationship with the Hercynian alkaline intrusions (Nie and Wu, 1998).

2.1. Stratigraphic sequences

The oldest stratigraphic unit exposed in the district is the Archean Jining Group, which occurs mainly in the southernmost parts of the district. It is approximately 8-km thick, and comprises mainly granulite, gneiss, amphibolite, marble, magnetite–quartzite and charnockite, The amphibolite has yielded an U–Pb zircon age of 2650 ± 89 Ma (Zhang, 1991), which is interpreted to be approximately the metamorphic age. A fault contact between the Jining Group and its overlying Wulashan Group has been observed (Shen et al., 1990; Zhang, 1991) (Table 1).

The Archean Wulashan Group mainly crops out in the southern part of the district, and consists of amphibolite, gneiss, granulite, magnetite quartzite and marble. Locally, magmatization is well developed in the group (up to migmatitic granite). The total thickness of the group is about 5 km (Table 1).

The metamorphic grade of both Archean Jining and Wulashan Groups varies from lower amphibolite to granulite facies. Compositionally, various granulite, amphibolite and gneiss of these two groups are closely similar to respective Archean rocks of the Qianxi Group of eastern Hebei (Jahn et al., 1987; Trumbull et al., 1992) and the Sanggan Group of northwestern Hebei (Nie, 1998). Zhang et al. (1999) suggested that the Jining Group belong to Orodos continental nucleus while the Wulashan Group represents a complete marine transgression cycle occurring in marginal basin developed to the north of the Orodos continental nucleus.

Archean to Paleoproterozoic granitoid stocks or dykes, which intrude the Jining and Wulashan Groups, yielded U–Pb zircon ages of 2470 ± 22 and 2521 ± 13 Ma (Zhang, 1989, 1991; Shen et al., 1990).

Proterozoic metamorphosed volcanics and sediments of the Sertengshan and Erdaowa Groups are sporadically distributed in the central parts of the district. The Sertengshan Group, with a total thickness of 2.8 km (Table 1), consists of gneiss, amphibolite, quartzite, mica–quartz schist and marble. It was formed in a pericontinental oceanic basin during a time period of 2200 to 2500 Ma (Shen et al., 1990; Wang et al., 1992). Meanwhile, the Erdaowa Group comprises mainly marine volcanics, flysch-type clastic sediments and carbonates with a total thickness of 1.5 km. It was deposited in fault-bounded basins during a time period of 2160 to 1840 Ma (Bai et al., 1996) (Table 1). It has been noted that both Sertengshan and Erdaowa Groups were folded and metamorphosed at low amphibolite to greenschist facies, and were ultimately incorporated into the Ordos continental nucleus (Wang et al., 1992; Zhang et al., 1999).

The Mesoproterozoic Chaertai and Bayan Obo Groups are located mainly in the north and northwest parts of the district. The Chaertai Group is composed mainly of schist, magnetite–quartzite, granulite and marble, with a total thickness of 4.5 km. Wang et al. (1992) suggested that these metamorphosed sediments were formed around 1600 Ma, and were deposited along the eastern margin of a fault-bounded basin (the so-called Langshan–Zhaertai graben) (Table 1). Mesoproterozoic clastic, carbonate and alkaline volcanic rocks of the Bayan Obo Group crop out mainly in the north and northwest portions of the district. The whole sedimentary sequence of the Group has an aggregate thickness of 8.2 km (Table 1), and is divisible in ascending order into 18 lithological units (Drew et al., 1990; Yuan et al., 1992; Bai et al., 1996). Nb–REE–Fe mineralization of the well-known Bayan Obo deposit occurs in between the Y8 and Y9 units whereas gold-bearing quartz veins of the Saiyinwusu deposit are hosted either by Y7 sandstone or Y9 carbonaceous slate and shale. The domination of clastic rocks of the group indicates rapid sedimentation in intensely basinal setting, the so-called Bayan Obo marginal rift (Wang et al., 1992; Zhang et al., 1999). Monazite separated

Table 1

Precambrian Crustal Evolution of the Baotou−Bayan Obo district, Inner Mongolia (modified from Shen et al., 1990; Nie and Bjoørlykke, 1994)

Group	Jining Group	Wulashan Group	Sertengshan Group	Erdaowa Group	Chaertai Group	Bayan Obo Group
Age (Ma)	More than 3000	2600-2700	2500-2200	2160-1840	1600	1500
Lithological association of metamorphic strata	Granulite, marble, Mag-quartzite; amphibolite, gneiss, & charnockite	Granulite, Px-Tr marble, gneiss; Migmatite; Mag-quartzite & amphibolite	Gneiss; marble; quartzite; Qtz schist; greenschist; amphibolite & felsic schist	Greenschist;gneiss; marble; felsic schist; Mag-quartzite & gneiss	Greenschist; felsic schist; carbonate sandstone, slate & quartzite	Quartzite, sandstone, carbonaceous slate, siltstone, carbonate, greenschist & felsic schist
Thickness (m)	8000	5000	2800	1500	4500	8200
Protoliths of metamorphic rock	Volcanics, clastic, carbonate & argillo-arenaceous sediments intercalated with BIF	Mafic volcanics, volcaniclastics & intrusions; clastic & carbonate, locally with BIF	Mafic to intermediate volcanics as well as argillaceous to argillo-arenaceous sediments	Mafic to intermediate volcanics as well as flysch type clastic sediments	Mafic to alkaline volcanics, clastic, carbonate, & argillite sediments	Mafic to intermediate volcanics, clastic, carbonate & argillite sediments
Geol. setting	Epicontinental shelf	Continental marginal basin	Fault depression basin	Fault-bounded basin	Continental rifting basin	Continental rifting basin
Metamorphic mineral assembalge	St-Alm-Bt-Ms-Qtz; Hbl-Pl-Bt; Bt-Hbl-Ep-Pl-Qtz; Cal-Tr-Qtz	Bt-Gr-Crd-Alm-Qtz; Di-Hbl-Bt-Qtz; Alm-Hbl-Di-Pl-Bt; Alm-Bt-Pl-Qtz	Di-Hy-Hbl-Pl-Qtz; Di-Hy-Pl-Hbl-Bt-Qtz; Chl-Epi-Hbl-Pl-Qtz	Ms-Chl-Ab-Qtz; Chl-Ep-Qtz-Cal; Chl-Qtz-Cal; Ep-Ab-Qtz	Chl-Ms-Act-Ab-Ep; Ms-Ep-Ab-Qtz; Ep-Bt-Crd-Qtz; Hbl-Ep-Pl-Qtz	Pum-Chl-Qtz; Zo-Act; Pmp-Act-Qtz; Prh-Chl
Metamorphic grade (phase)	Granulite to high amphibolite	Medium to high amphibolite	High greenschist to low amphibolite	Low to high green-schist	Low to high green-schist	Prehnite-pumpellyite to low greenschist
P-T conditions	T = 729°-849°C; P = 0.5-1.0 GPa	T = 690°-760°C; P = 0.5-0.8 GPa	T = 550°-650°C; P = 0.5-0.7 GPa	T = 400°-500°C; P = 0.4-0.5 GPa	T = 350°-500°C; P = 0.3-0.5 GPa	T = 300°-400°C; P = 0.1-0.2 GPa
Magmatic actrivity & migmatization	Tonalite → Diorite porphyrite dykes → Granitoid batholiths and stocks → Alkaline mafic and syenite dyke swarms and stocks → Migmatization of various metamorphic rocks →					

Abbreviations: Alm = almandine; Ab = albite; Act = actinolite; Bt = biotite; Cal = calcite; Chl = chlorite; Crd = cordierite; Di = diopside; Ep = epidote; Gr = graphite; Hbl = hornblende; Hy = hypersthene; Mag = magnetite; Ms = muscovite; Pl = plagioclase; Pmp = pumpellyite; Prh = prehnite; Px = pyroxene; Qtz = quartz; St = staurolite; Tr = tremolite; Zo = zoisite.

from volcano-sedimentary rocks of the group yields Sm–Nd and U–Pb isotope ages of about 1400 to 1500 Ma (Nakai et al., 1989).

Paleozoic marine sediments and Mesozoic subaerial volcano-sedimentary rocks are sporadically distributed in the central and northern parts of the district owing to intensive erosion during several uplift events (Shen et al., 1990; Bureau of Geology and Mineral Resources of Inner Mongolia, 1991, Fig. 1). The Paleozoic volcano-sedimentary sequences occurring in the northernmost part of the district constitute part of the broader Mongolian–Great Hinggan fold belt between the North China craton and Siberian (or Angara) platform (Wang and Liu, 1991; Wang et al., 1992; Sengor and Natal'in, 1996). Mesozoic volcanic and continental sedimentary rocks (Shiguai, Bainuyangpan and Guyang Groups), mainly of Jurassic to Early Cretaceous age, occur primarily in basins developed unconformably on the Precambrian metamorphic rocks. The volcanic rocks are composed of andesitic, dacitic tuff and flow-banded rhyolite. Several small-scale Cenozoic sedimentary basins with placer gold are also identified in the district.

2.2. Tectonics

Precambrian stratigraphic units in the district are strongly folded and faulted (Li et al., 1990; Wang et al., 1992; Nie and Bjørlykke, 1994; Zhang et al., 1999). The axes of these folds are generally WE- to NE-trending. Numerous WE-, NE- and NW-trending faults are present, among which four most prominent fault systems are recognized: Daqingshan–Wulashan, Shetai–Guyang–Wuchuan, Chuanjing–Bulutai, and Dahuabei–Hejiao–Damao Faults. These four fault systems are integral to understand the gold metallogeny of the Baotou–Bayan Obo district. The faults control the spatial distribution of alkaline igneous rock bodies and major gold deposits (Geological Institute of Inner Mongolia, 1990; Zhang et al., 1999). The basic features of some of these faults are briefly described here.

The Daqingshan–Wulashan fault zone is located in the southernmost part of the district and formed a part of the WE-trending Baotou–Huhhot deep-seated fault belt (Meng, 1986; Zhang, 1989; Hu et al., 1990; Davis et al., 1998). It also defines the boundary of the Inner Mongolian axis to the north and Ordos depression to

the south (Bureau of Geology and Mineral Resources of Inner Mongolia, 1991; Chen et al., 1996). This zone, consisting mainly of mylonite, tectono-clastic rocks, tectonic lenses and breccia, is thought to have been formed by a large nappe movement during the Late Archean to Paleoproterozoic time period (Meng, 1986; Hu et al., 1990; Wu, 1993). During the Hercynian (350–300 Ma) tectonic events, reactivation of this fault zone resulted in thrusting of the Archean high-grade metamorphic rocks onto the Meso- to Neoproterozoic and Early Paleozoic volcano-sedimentary sequences (Wu, 1993). Post-thrust extension tectonic event was probably the cause of the emplacement of the Late Hercynian (285–290 Ma) alkaline intrusions, which are well developed along the Daqingshan–Wulashan fault zone. Geophysical data indicate that the fault belt reaches to the Moho; small-scale earthquakes along the belt have been recorded during the past 10 years (Hu et al., 1990; Wu, 1993). The Wulashan deposit is situated on the northern side of the Daqingshan–Wulashan fault zone (Meng, 1986; Zhang, 1989; Hu et al., 1990; Chen et al., 1996).

Situated in the central part of the district, the WE-trending Shetai–Guyang–Wuchuan shear zone is about 5- to 10-km wide and several hundreds of kilometers long. It separates the Palaeoproterozoic Sertengshan, Erdaowa Groups, Mesoproterozoic Chaertai and Bayan Obo Groups to the north, from the Archean Jining and Wulashan Groups to the south. Metamorphism, igneous activity and gold metallogeny in the south and central parts of the district are mainly controlled by this shear zone (Li et al., 1990; Zhang, 1991). The structural geology of the northernmost portion of the district, especially in the Bayan Obo–Saiyinwusu area, is complex. During the Permian, a continent-to-continent collision intensively deformed the passive margin on the northern edge of the North China craton (Wang and Liu, 1991; Wang and Mo, 1995). This deformation resulted in the formation of the Chuanjing–Bulutai deep-seated fault belt, which is 15–30-km wide and 250-km long. It constitutes a part of Junggar–Hinggan Fault (Miller et al., 1998), and divides the study area into two tectonic units: the North China craton to the south and the Tianshan–Mongolia–Hinggan Paleozoic geosynclinal belt to the north. Numerous fault melanges, thrust and reverse faults, large-scale fold and basement horses are well developed along this fault belt (Drew

et al., 1990; Bai et al., 1996). The WE- and NE-trending faults show a close relationship with gold mineralization. The Dahuabei–Laoyanghao–Bayan Obo (also called Dahuabei–Hejiao–Damao fault) fault strikes in NE direction, and extends more than 300 km. It is a most prominent NE-trending fault, and was formed during Late Paleozoic to Early Mesozoic time (Geological Institute of Inner Mongolia, 1988; Nie and Bjørlykke, 1994). A great number of Hercynian, Indosinian and Yanshanian alkaline and high K granitoids intrude this fault. Most of the gold deposits described in this paper occur at or near intersections between this fault and the WE-trending faults. In addition, small and discontinuous NE- WE- and NW-trending lineaments are also evident from air photo analyses.

2.3. Intrusions

Mafic to granitoid batholiths, stocks and dykes are common throughout the Baotou–Bayan Obo district. Most of these Proterozoic intrusions crop out in the southern part of the district, and comprise monzonite, gneissose diorite, monzonitic granite and K-feldspar granite. They range from isolated stocks to multiphase batholiths, up to 120 km^2 in the area. All these Proterozoic rock bodies intrude the Archean metamorphic rocks of the Jining and Wulashan Groups, and are cut by Mesozoic granite dykes (Shen et al., 1990; Bureau of Geology and Mineral Resources of Inner Mongolia, 1991; Nie et al., 2000). It is noted that a great number of pegmatite dykes showing a highly evolved mineralogy (K-feldspar and quartz) crop out along the northern side of the Daqingshan–Wulashan fault belt. Zircon extracted from two of these Proterozoic monzonite stocks yields two U–Pb isotopic ages of 1997 ± 6 and 1999 ± 19 Ma, respectively (Wang et al., 1992).

Hercynian alkaline intrusive stocks and dyke swarms occur frequently in the district. They are composed of alkalic melagabbro, leucogabbro, aegirine–augite syenite, monzonite and high K granite. All these igneous rock bodies intrude Precambrian metamorphic rocks, and yield U–Pb zircon ages ranging from 302 to 249 Ma. In the central and southern portions of the district, aegirine–augite syenite and monzonite are widely distributed along the fault and fracture zones occurring in the Precambrian metamor-

phic rocks as irregular stocks, dykes swarms and lenses. The most important intrusions are the Wulashan syenite dyke swarm, Donghuofang syenite porphyry and Baotoudong syenite stocks. The first two bear close spatial relationship, as host and wall rocks, to the gold mineralization. Gold, antimony, arsenic, barium, and tellurium anomalies have also been outlined in the Baotoudong syenite stock with an outcrop of 10 km^2. The aegirine–augite syenite dykes and lenses commonly constitute WE-trending intrusive dyke swarms, each one of them has an outcrop of less than 0.5 km^2, except for the Baotoudong stock. The red-colored fine-grained syenite consists mainly of 72–83% K-feldspar, 7–10% quartz and 4–9% aegirine-augite. Accessory minerals are magnetite, pyrite, apatite and monazite. A number of alkalic melagabbro, leucogabbro and meladiorite stocks and dykes widely crop out in the vicinity of the Shibaqinhao, Laoyanghao, Saiyinwusu and Houshihua gold deposits. Since ^{40}Ar/^{39}Ar data on the hornblende and K-feldspar separates from these intrusive stocks and dykes range from 302 to 249 Ma, it seems likely that these intrusions formed during Hercynian orogeny. The same or similar isotopic age range (Table 4) of the alkaline intrusions and gold ores indicate that a close genetic relationship exists between the Hercynian alkaline magmatism and gold deposition at Shibaqinhao, Laoyanghao and Houshihua, respectively.

Indosinian granitoid batholiths and stocks mainly occur in the central part of the district, and intrude the Precambrian metamorphic rocks and Hercynian alkaline igneous bodies, and were cut by Mesozoic Yanshanian mafic to felsic intrusive dykes. Mesozoic Yanshanian granite and K feldspar granite batholiths as well as a great number of diorite porphyry, aplite, pegmatite and diabase dykes have also been reported in the central and northern portions of the district.

3. Methods

3.1. Sampling

Deeply inclined and continuously cored drill holes extending below the limit of weathering for Wulashan, Donghuofang and Shibaqinhao were systemati-

Table 2
Basic geological features of major gold deposits in the Baotou–Bayan Obo area, Inner Mongolia

Deposit, County	Tectonic setting	Host rocks (time)	Intrusives (Ma)	Orebody	Metallic mineral	Alteration	Deformation	Grade (g/t), reserve/utility	References
Hosted by Archean high-grade metamorphic rocks									
(1) Shibaqinghao, Guyang	Shear zone in Ar terrain	Amph, gneiss, schist, migmatite (Ar) and mafic porphyry stock or dyke (Pz)	Diorite, gabbro, mafic porphyry stock and dyke (265 ± 4 Ma)	NW- or WE-trending Qtz or Qtz–Cc veins and veinlet groups	Py, Cpy, Gn, Mo, Ilm, Mag, Lm, Hem, native Au and Ele	Qtz, Kfs, Bt, Ser, Act, Chl, Epi and Cc	Strongly deformed	2–10 (up to 150) (ave. 7), M/Min	Zhang, 1991; Nie et al., 2000
(2) Laoyanghao, Guyang	Shear zone in Ar terrain	Hbl–Pl gneiss, schist migmatite (Ar) and gabbro or other mafic dykes (Pz)	Granitoids, mafic and gabbro porphyry dykes (265 ± 6 Ma)	NW-trending Qtz vein and veinlet groups	Py, Cpy, Bn Gn, Lm, native Au, Ele	Qtz, Bt, Ser, Cc, Chl and Epi	Deformed	3–25 (up to 126) (ave. 10), M/Min	Zhang, 1991
(3) Houshihua, Wuchuan	Shear zone in Ar terrain	Gneiss, migmatite, schist, and marble (Ar) and mafic porphyry (Pz)	Tonalite (Pt), granite (Mz) and mafic porphyry (306 ± 6 Ma)	NE-trending Qtz veins, veinlet groups and altered Myn	Py, Cpy, Gn, Sph, Mo, Apy, Alt, Lm, native Au, Cala, Pet, Mel and Hes	Qtz, Kfs, Ser, Chl, Epi and Cc	Strongly deformed	5–37 (up to 152) (ave. 8), S/Min	Chen et al., 1996
Hosted by Proterozoic sedimentary rocks									
(4) Saiyinwusu, Darhan Muminggan Joint Banner	Marginal graben of Ar terrain	Quartzite, black slate, schist, limestone, sandstone (Pt) and leucogabbro (Pz)	Granitoid (Mz) and leucogabbro dyke or stock (249 ± 5 Ma)	WE- to NW-trending veins, veinlet groups and altered Myn	Py, Mar, Apy, Cpy, Gn, Sph, Got, Lm, Hem Ele and native Au	Qtz, Ser, Mc, Cc, Kln, Mus, Ili, Epi and Chl	Strongly fractured	5–50 up to 170 (ave. 10), M/Min	Zhang, 1991
(5) Motianling, Wuchuan	Faulted basin of the Ar and Pt terrain	Silicified marble and Ser-Chl phyllite (Pt)	Alkaline syenite dyke (270 ± 5 Ma)	NS-trending veins, layers and tabular bodies	Py, Cpy, Apy, Sph, Lm, native Au and Ele	Qtz, Cc, Ser, Chl and Lm	Strongly fractured	2–15 (ave. 5), S/Exp	Chen et al., 1996

Hosted by or related to Hercynian alkaline intrusive rocks

(6) Wulashan, Baotou City	Sheared and fractured zones in the Ar terrain	Amp, granulite, Mag-migmatite, gneiss, quartzite (Ar) and alkaline syenite dykes or stocks (Pz)	Bt-granite and alkaline syenite dyke or stock (299 ± 3 and 298 ± 5 Ma)	WE to NE-trending Qtz or Qtz–Kfs veins and veinlet groups	Py, Cpy, Gn, Sph, Apy, Mag, native Au, Ele, Cala, Lm, Mel, Pet, Alt, Sd, Bmt, Hem and Spe	Qtz, Mc, Or, Ser, Chl, Px, Cc, Ank and Epi	Deformed	5–30 (up to 353) (ave. 7), L/Min	Zhang, 1991; Guo, 1992
(7) Donghuofang, Wuchuan	Shear zone in Ar terrain	Gneiss (Ar), granitoid (Pt), breccia pipe, monzonite and alkaline syenite stock (Pz)	Monzonite (280 ± 4 Ma) and alkaline syenite (276 ± 5 Ma, (278 ± 4 Ma)	NE- NW- or WE-trending Qtz veins, vein groups or fractured zone	Py, Gn, Sph, Cpy, Bn, Chc, Mal, Cov, native Au, Cala, Ele, Alt, Hes and Tbm	Qtz, Kfs, Ser, Chl, Cc, Ank and Kln	Weak	3–18 (up to 138) (ave. 7), M/Exp	Chen et al., 1996
(8) Luchang, Tumd Zuoqi	Faulted zone in the Ar terrain	Gneiss, Amp, marble (Ar) and alkaline melagabbro (335 ± 3 Ma)	Qtz diorite, monzo-granite (Pt), diabase and gabbro (Pz)	NE-trending veins, veinlet groups and lenses	Cpy, Sph, Po, Gn, Mar, Cpy, Bn, native Au, Ele Cala and Alt	Qtz, Ser, Cc, Chl and Epi	Weak to intermediate fractured	2–28 (up to 78) (ave. 8), M/Min	Shen Baofeng, written communication, 2000

Abbreviations: Ab = albite; Alt = altaite; Amph = amphibolite; Ank = ankerite; Ap = apatite; Apy = arsenopyrite; Ar = Archean; Bar = barite; Bmt = bismuthinite; Bn = bornite; Bis = bismuthine; Bt = biotite; Cala = calaverite; Cc = calcite; Chc = chalcocite; Chl = chlorite; Cpy = chalcopyrite; Cov = covellite; Cz = Cenozoic; Diss = disseminated; Ele = electrum; Ep = epidote; Gn = galena; Got = goethite; Grt = garnet; Hbl = hornblende; Hem = hematite; Hes = hessite; Ilm = ilmenite; Kfs = K-feldspar; Kln = kaolinite; Lm = limonite; Mag = magnetite; Mar = marcasite; Mc = microcline; Mal = malachite; Mel = melonite; Mo = molybdenite; Mus = muscovite; Myn = mylonite; Mz = Mesozoic; Or = orthoclase; Pet = petzite; Pl = plagioclase; Po = pyrrhotite; Pt = Proterozoic; Px = pyroxene; Py = pyrite; Pz = Paleozoic; Q = Quarternary; Qtz = quartz; Rut = rutile; Sch = scheelite; Sd = Siderite; Ser = sericite; Spe = specularite; Sph = sphalerite; Syl = sylvanite; Tbm = tellurbismuth; Tet = tetraedrite; Tur = tourmaline; Wol = wolframite; Zrn = zircon.
The deposit numbers correspond to those in Fig. 1; Au and Ag in g/t; L = large scale with gold production of more than 20 t; M = middle scale with gold metal between 5 and 20 t; S = small scale with gold metal less than 5 t; Min = mining; Exp = explored or under mineral exploration.
Gold reserve of each gold deposit is taken from National Administrative Bureau of Gold and Ministry of Metallurgical Industry (MMI).

cally logged and sampled. A number samples for sulfur and lead isotope analysis were taken from relatively short vertical drill holes at Laoyanghao, Saiyinwusu and Houshihua. The whole rock samples of these alkaline intrusions were collected from well-exposed outcrops. Each sample consisted of four to five blocks (3−5 kg) taken within 2−5 m of each other. All the minerals used for sulfur and lead isotope analyses were separated from hand specimens by conventional preparation techniques involving crushing, an oscillating table, heavy liquid and a magnetic separator. All mineral separates (galena, pyrite and pyrrhotite) were further purified by hand-picking to at least 96% purity.

3.2. Analytical techniques

Whole rock samples were analyzed by X-ray fluorescence spectrometry and atomic absorption spectrophotometry. Ferrous iron was determined by digesting the sample in a mixture of HF and H_2SO_4 and titrating against a standard solution of potassium dichromate. Trace element (Rb, Sr, Ba, Th and U) analyses were carried out by the INAA method. All these analyses were performed at School of Earth Sciences, La Trobe University, Australia.

The sulfur isotope compositions for the galena, pyrite and pyrrhotite were determined by a MAT230 mass spectrometer at Institute of Geology, Chinese Academy of Geological Sciences and Isotope Laboratory of the Changchun College of Geology. Routine analytical precision for standard material was ± 0.2‰. Chemistry and mass spectrometer procedures are described by Nie (1993).

For lead isotope analyses, separated galena, pyrite and pyrrhotite were dissolved in 2 ml 2N HCl and further purified either by fractional crystallization, or for an Fe-rich sample, by an ion exchange column that yielded $PbCl_2$ of high purity. The lead was placed on a Re filament together with a solution of silica gel and phosphoric acid. Separation of U and Pb from pyrite and pyrrhotite involved anion exchange chromatography in a HBr solution, followed by anodic electro-deposition in dilute HNO_3. The total systematic laboratory blank of 6 to 8 ng was not significant in this Pb isotope study. The 2σ variations are 0.1%, 0.09% and 0.30% for the $^{206}Pb/^{204}Pb$, $^{207}Pb/^{204}Pb$ and $^{208}Pb/^{204}Pb$ ratios, respectively (Birkeland, 1990).

4. Basic geologic features of the gold deposits

Gold mineralization is widely distributed in the Baotou−Bayan Obo district, and up to the present, above 52 gold deposits and prospects have been identified. All these deposits and prospects can be classified into three categories: (1) hosted by the Archean high-grade metamorphic rocks; (2) hosted by Proterozoic sedimentary rocks; (3) hosted by or related to Hercynian alkaline intrusions. It is noteworthy that most of these gold deposits occur in the Precambrian metamorphic rocks and show an intimate spatial tie with the Hercynian alkaline intrusions. The tectonic setting, deposit geology, geochemistry and mineralogy differ from deposit (or prospect) to deposit (or prospect). The basic geologic features of major gold deposits and prospects are presented in Table 2.

4.1. Gold deposits hosted by Archean high-grade metamorphic rocks

4.1.1. Shibaqinhao deposits, Guyang

The Shibaqinhao deposit is located 38 km west of the Guyang Town (Figs. 1, 2). It was discovered in the middle of 1980s, and gold production started in 1991, with annual gold production of 15,000 oz. The deposit has known reserves of 2 Mt of ore, with an average grade of 7 g/t Au (Table 2).

The Shibaqinhao area is situated in the western portion of the WE-trending Shetai−Guyang−Wuchuan faulted shear zone. WE- and NW-trending faults and fractures are well developed, and are considered as the main controlling factors of gold mineralization. The host rocks of the deposit are composed mainly of Archean amphibolite, biotite−plagioclase gneiss, hornblende−plagioclase gneiss and mafic porphyry. Gneissic banding of these metamorphic rocks with amphibolite facies strikes 280° to 300°, and dips 72° to 85° toward NE or SW. Narrow lenses of banded iron-formation occur within the amphibolite around the gold mine. Mafic porphyry dykes and stocks are widely exposed in the central part of the mineralized area, and constitute the wall rocks of the ore bodies. The dark-colored mafic porphyry is characterized by clinopyroxene, hornblende and plagioclase phenocrysts. The groundmass is typically composed of fine-grained (< 0.1 mm) plagioclase, hornblende, clinopyroxene, chlorite, apa-
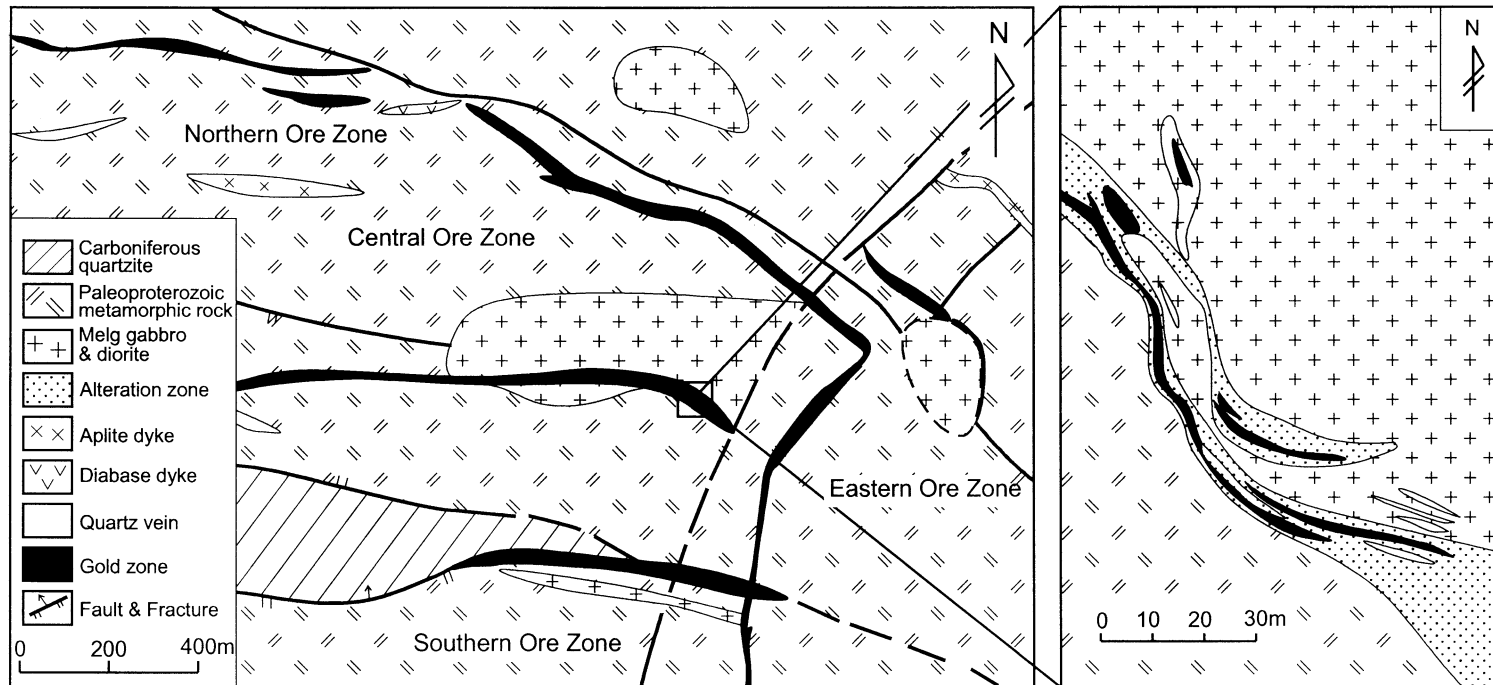
Fig. 2. Schematic geological map of the Shibaqinhao gold deposit. Insets of the southeastern part of the central gold ore zone.

tite and magnetite. Chemical analyses for major and trace elements in three mafic porphyry samples are listed in Table 3. They plot in the trachyte field on the total alkali vs. silica (TAS) diagram (Fig. 3) and show some shoshonitic affinities on the $K_2O\%$ vs. SiO_2 diagram (Fig. 4). $^{40}Ar/^{39}Ar$ isotopic dating on hornblende from the mafic porphyry stock gave an age of 265 ± 4 Ma (Table 4).

The main loci of gold mineralization at Shibaqinhao are WE- and NS-trending retrograde shear zones in which chlorite and sericite schist are developed. A lot of contorted and irregular quartz and calcite veins were identified in the Archean gneiss and amphibolite. To date, four gold mineralized zones have been delineated: northern, central, southern and eastern zones (Fig. 2), of which the northern and central are the most important ones, and are briefly described as follows.

(1) Northern zone: Located at northern portion of the district, it is 257-m long, 15- to 50-m wide with proven vertical depth of 220 m. It strikes 330°, and dips 70° to 80° toward NE. The host rocks consist of migmatite, biotite–plagioclase gneiss, sericite–quartz schist and amphibolite.

(2) Central zone: It is composed of mylonite, schist and Hercynian mafic porphyry stock, and ranges from 1400- to 2000-m long, and 14- to 40-m wide. It is the largest mineralization zone in the district. The whole zone strikes WE, and dips 72° to 85° towards north or south. The Archean metamorphic wall rocks to the ore bodies are biotite–plagioclase gneiss and amphibolite, and were intruded by Hercynian alkaline mafic porphyry stocks or dykes.

Several gold anomalies are also delineated in the southern and eastern zones. These anomalies relate to low grade, small-scale and discontinuous gold veins.

The main sources of gold ores at Shibaqinhao are No. 1, 2, 3, 4, 5 and 6 ore bodies, of which five occur within the central zone, and one in the northern zone.

Table 3
Whole rock major and trace element compositions of least altered samples from the major Hercynian alkalic intrusions associated with gold deposits in the Baotou–Bayan Obo district, Inner Mongolia

Sample	SQ9901	SQ9902	SQ9903	LY9901	LY9902	SS9901	SS9902	HD9901	HD9902	HD9903	D9901	D9902	D9903
No.[a]	1	2	3	4	5	6	7	8	9	10	11	12	13
Rocks	MP	MP	MP	MG	MG	LG	LG	AAS	AAS	AAS	Syenite	Syenite	Syenite
Major elements (wt.%)													
SiO_2	49.93	49.28	49.85	51.03	52.12	53.93	53.34	62.11	64.24	64.54	59.74	58.69	59.23
TiO_2	0.84	1.05	1.02	1.25	0.98	0.66	0.56	0.28	0.15	0.65	1.06	0.57	0.43
Al_2O_3	17.34	16.12	16.56	16.30	16.00	16.64	16.90	17.65	17.22	15.57	17.58	16.94	16.67
TFeO	7.53	7.66	7.19	6.09	6.02	7.06	7.93	4.26	3.62	3.63	4.41	4.32	3.43
MnO	0.24	0.18	0.16	0.18	0.14	0.17	0.16	0.08	0.07	0.07	0.12	0.13	0.15
MgO	4.21	6.03	5.53	5.73	5.99	3.04	3.41	1.32	1.45	1.21	2.16	1.47	2.38
CaO	8.32	9.32	8.63	7.64	7.87	6.96	6.92	2.94	1.99	2.04	3.09	3.85	3.03
Na_2O	4.23	4.63	5.32	4.77	4.65	5.44	5.11	3.66	4.34	3.95	4.06	4.26	4.87
K_2O	2.43	3.75	3.87	3.92	3.76	3.33	3.07	5.26	5.13	5.42	4.24	4.40	5.13
P_2O_5	0.57	0.36	0.28	0.57	0.45	0.51	0.84	0.15	0.09	0.33	0.34	0.23	0.33
CO_2	3.12	0.27	0.26	0.74	0.65	0.46	0.71	0.55	0.44	0.99	1.23	3.73	2.87
LOI	1.45	1.06	1.23	1.44	1.30	1.99	1.03	1.30	0.32	0.95	1.15	1.42	1.21
Total	100.21	99.71	99.90	99.66	99.93	100.19	99.98	99.56	99.06	99.35	99.18	100.01	99.73
Trace elements (ppm)													
Sr	750	439	489	423	503	320	342	130	134	167	135	116	125
Rb	65	74	52	67	77	99	102	98	101	110	141	155	204
Ba	676	576	620	780	860	523	479	1382	1630	2891	2067	1315	1328
U	2.0	2.0	2.5	3.4	4.2	2.9	3.6	2.2	3.2	3.4	2.6	3.2	3.8
Th	8.4	3.6	7.0	6.8	5.8	7.3	6.9	4.8	5.3	4.7	4.9	4.3	4.8

Abbreviations: AAS = aegirine–augite syenite; LG = leucogabbro; LOI = loss of volatile components; MG = melagabbro; MP = mafic porphyry; TFeO = FeO + Fe_2O_3.
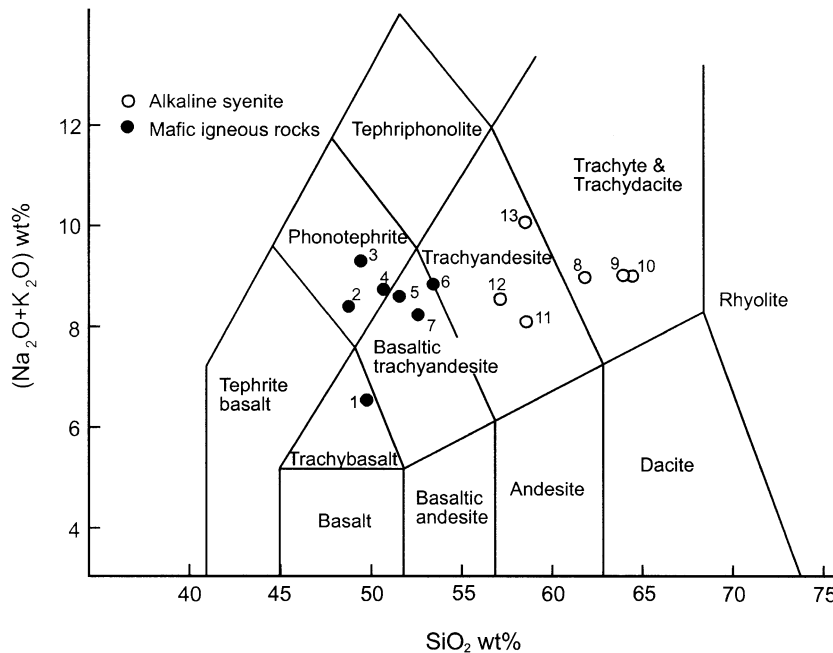[a] Number corresponds to these sample data on Figs. 2 and 3.

Fig. 3. Total alkali ($K_2O + Na_2O$ wt.%) vs. SiO_2 wt.% diagram for these Hercynian alkaline intrusions associated with gold deposits occurring in the Baotou–Bayan Obo district. (1–3) Shibaqinhao mafic porphyry dykes; (4–5) Laoyanghao melagabbro and leucogabbro dykes; (6–7) Saiyinwusu leucogabbro dykes; (8–10) Wulashan aegirine–augite syenite stocks; (11–13) Donghuofang syenite stocks.

These ore bodies vary from 98- to 280-m long, and 1.5- to 4-m wide, with a decline depth of 350 to 400 m. The gold content ranges from 2 to 10 g/t, with an average value of 7 g/t. Each of these orebodies is composed mainly of gold-bearing quartz and quartz–calcite veins, and disseminated-veinlet in altered-fractured rocks. All these veins and veinlets cut the altered Archean metamorphic rocks, but some of them are hosted by the mafic porphyry stocks or dykes. At some localities, the quartz veins discordant with the foliated wall rocks. The veins are locally massive, commonly ribboned near their contacts with altered wall rocks, and contain slab-shaped inclusions of intensely altered and pyritized host rocks. These slab-shaped inclusions locally result in a breccia-vein appearance. Mineralogical constituents of the gold ores and alteration zones at Shibaqinhao are listed in Table 2. $^{40}Ar/^{39}Ar$ isotopic dating on the sericite separates from the gold ores yields an age of 247 ± 4 Ma (Table 4). It has been suggested that the gold mineralization is essentially contemporaneous with the emplacement of the Hercynian alkaline mafic porphyry.

4.1.2. Laoyanghao deposit, Guyang

The Laoyanghao deposit is located 30 km northwest of the Guyang town, and 15 km southwest of Hejiao village (Fig. 1). The deposit was discovered in the mid 1980s during regional geological mapping (1:50 000) by No. 1 Geological Party of Inner Mongolian Bureau of Geology and Mineral Resources. The deposit has been explored by 15 diamond drill-holes, and a series of tunnels. It has a reserve of 3 t gold, with an average grade of 7 g/t gold. A local government mine has been established, and gold production started in 1994, with an annual production of 270 kg Au.

The Laoyanghao deposit is situated in the western portion of the WE-trending Shetai–Guyang–Wuchuan fault belt. The host rocks of the deposit consist of Archean hornblende–plagioclase gneiss, chlorite–quartz schist and melagabbro. The structural style at the Laoyanghao deposit and its surroundings is dominated by a series of torsion faults and schistosity (altered-fractured or shear zones) (Fig. 5). Two parallel NW-trending schistosity zones (west and east) are the most important ones, and bear a close relation to gold mineralization. They appear to be flexed and bent at
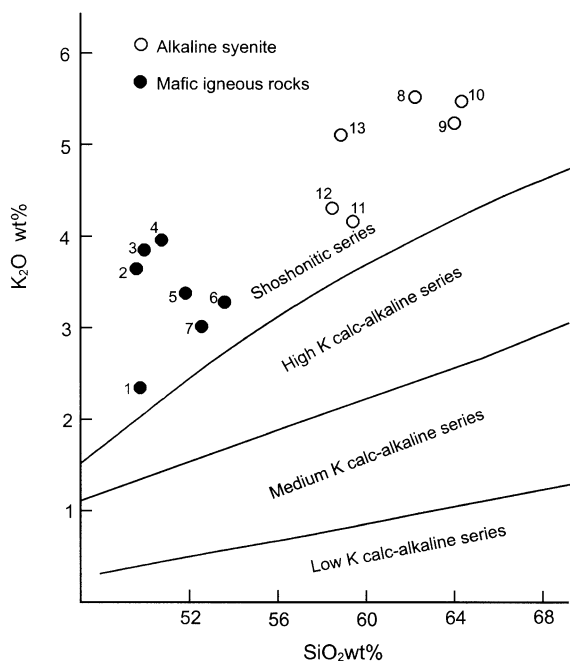
Fig. 4. K_2O wt.% vs. SiO_2 wt.% diagram for these Hercynian alkaline intrusions associated with gold deposits occurring in the Baotou–Bayan Obo district. (1–3) Shibaqinhao mafic porphyry dykes; (4–5) Laoyanghao melagabbro and leucogabbro dykes; (6–7) Saiyinwusu leucogabbro dykes; (8–10) Wulashan aegirine–augite syenite stocks; (11–13) Donghuofang syenite stocks.

southeast end. The zones consist mainly of selvage, slip veins and breccias ranging from 9- to 2400-m long, and 13- to 55-m wide, with a downdip extent of 300 to 500 m, and are cut by NE-trending faults (Fig. 5).

Mafic to granitoid stocks and dykes occur frequently in the Laoyanghao district. The most important intrusions are mafic porphyry and melagabbro stocks and dykes, which intrude the Archean metamorphic rocks. Some of these melagabbro dykes constitute the footwall of the ore bodies, and are cut by mafic porphyry stocks and melagabbro dykes. The dark-colored intrusions are characterized by fine- to medium-grained clinopyroxene, plagioclase and hornblende. When the whole rock analytical data (Table 3) plotted on the total alkali-silica diagram (Fig. 3) and the K_2O (wt.%) vs. SiO_2 (wt.%) diagram (Fig. 4), the mafic porphyry and melagabbro samples scatter within the alkaline igneous rock range. Dating of hornblende from the melagabbro dyke gave an $^{40}Ar/^{39}Ar$ age of 258 ± 3 Ma (Table 3).

Gold mineralization occurs mainly within the western and eastern schistosity zones as gold-bearing quartz veins and altered-fractured rocks. To date, seven ore bodies have been identified in the eastern zone. All these ore bodies show variable length of 15 to 80 m and thickness of 0.2 to 3 m. The down-dip extent of these ore bodies varies from 15 to 120 m. All of them dip 65° to 74° to NE, and have ore grade of 3 to 25 g/t, with an average value of 6 g/t. Some gold-bearing quartz veins are also observed within mafic porphyry stocks or dykes. The highest gold grades occur in pyrite gouge. Four ore bodies have been outlined in the western zone. The length of these ore bodies varies from 80 to 240 m, and the width from 2 to 3 m, with declined depth of 80 to 100 m. The ore bodies reportedly grade 5 to 15 g/t, with an average value of 10 g/t.

The mineralogy of gold-bearing quartz veins and altered-fractured rocks is relatively simple, and listed in Table 2. Isotopic age dating on the sericite from the gold ores yields an $^{40}Ar/^{39}Ar$ age of 256 ± 3 Ma (Table 4), which is close to that of the melagabbro dyke associated with the ore bodies.

4.1.3. Houshihua deposit, Wuchuan

The Houshihua deposit is located 52 km southwest of Wuchuan town (Fig. 1). It was discovered in the early of 1980s by No. 1 Geological Party of Inner Mongolian Bureau of Geology and Mineral Resources (IMBGMR) during a geological investigation. It has a reserve of 3 t gold with an average value of 8 g/t gold.

The Houshihua shear zone and its contained gold deposit lie in the eastern section of the Shetai–Guyang–Wuchuan faulted shear zone within the North China craton (Fig. 6). The strata exposed in the district comprise Archean hornblende–plagioclase gneiss, migmatite, garnet–biotite–chlorite schist, epidote–chlorite schist, biotite–hornblende schist, sericite–quartz schist and marble of the Wulashan Group. All these metamorphic rocks have been strongly fractured and sheared, varying from incipient mylonite and mylonite to ultramylonite. They may have formed during 2040 to 1648 Ma (Chen et al., 1996). Archean charnockite, Proterozoic peridotite, quartz diorite and migmatite, Hercynian mafic porphyry and Mesozoic Yanshanian granitoids are also well developed. Among these intrusions, the Hercynian mafic porphyry dykes commonly constitute the footwall or hanging-wall of the ore bodies. Petrologically,

Table 4

K–Ar and ^{40}Ar–^{39}Ar age data[a] of least altered alkaline intrusive and gold ore samples from major gold deposits in the Baotou–Bayan Obo district

Gold deposits	Age of alkaline intrusive rocks (Ma)	Age of altered rocks or gold ores (Ma)	References
Gold deposits hosted by Archean high-grade metamorphic rocks			
Shibaqinhao	239 ± 4 (K–Ar WR, high K Bt granite)	247 ± 4 (K–Ar WR, Kfs–Qtz–Ser rocks	Zhang et al., 1999
	254 ± 4 (K–Ar WR, pegmatite)	of FG granite)	
	265 ± 4 (^{40}Ar–^{39}Ar Hbl, M Porphyry)	264 ± 3 (^{40}Ar–^{39}Ar, Ser from gold-bearing Qtz vein)	Nie et al., 2000
Laoyanghao	266 ± 4 (K–Ar WR, Bt granite)	254 ± 4 (K–Ar WR, Qtz–Ser alt. rock)	Zhang et al., 1999
	258 ± 3 (^{40}Ar–^{39}Ar Hbl, M Porphyry)	256 ± 3 (^{40}Ar–^{39}Ar Ser, gold ore)	Nie et al., 2000
Houshihua	302 ± 6 (^{40}Ar–^{39}Ar Hbl, leucogabbro)	301 ± 5 (^{40}Ar–^{39}Ar Ser, gold ores)	Nie et al., 2000
Gold deposits hosted by Proterozoic volcano-sedimentary rocks			
Saiyingwusu	233 ± 3 (K–Ar WR, Bt granite)	197 ± 3 (K–Ar WR, alt. Bt granite)	Zhang et al., 1999
	249 ± 5 (^{40}Ar–^{39}Ar Hbl, leucogabbro)	249 ± 5 (^{40}Ar–^{39}Ar Ser, gold ores)	Nie et al., 2000
Gold deposits hosted by or related to Hercynian alkaline intrusions			
Wulashan	299 ± 5 (K–Ar WR, Kfs–Bt granite)	247 ± 6 (K–Ar WR, Qtz–Ser alt zone)	Zhang et al., 1999
	299 ± 3 (^{40}Ar–^{39}Ar Kfs, AA syenite)	297 ± 4 (^{40}Ar–^{39}Ar Ser, gold ores)	Nie et al., 2000
	298 ± 5 (^{40}Ar–^{39}Ar Kfs, AA syenite)	296 ± 4 (^{40}Ar–^{39}Ar Ser, gold ores)	
Donghuofang	278 ± 4 (^{40}Ar–^{39}Ar Kfs, AA syenite)	277 ± 4 (^{40}Ar–^{39}Ar Ser, gold ores)	Nie et al., 2000
	276 ± 5 (^{40}Ar–^{39}Ar Kfs, AA syenite)	276 ± 3 (^{40}Ar–^{39}Ar Ser, gold ores)	
	280 ± 4 (^{40}Ar–^{39}Ar Hbl, monzonite)		

Abbreviations: AA = aegirine–augite syenite; alt = alteration; Bt = biotite; FG = fine-grained; Hbl = hornblende; Kfs = K-feldspar; M = mafic; Ser = sericite; Qtz—quartz; WR = whole rock.

[a] ^{40}Ar–^{39}Ar ages were obtained from high-purity (>97%) mineral separates of K feldspar, sericite and hornblende from major gold deposits and associated alkaline intrusions. Isotopic analyses were carried out by AEI MS10 mass spectrometer at School of Earth Sciences, La Trobe University, Australia.

mineralogically and geochemically, the mafic porphyry is similar to the mafic porphyry stock occurring in the Shibaqinhao deposit (Figs. 3 and 4). $^{40}Ar/^{39}Ar$ isotopic dating on hornblende from the mafic porphyry gave an age of 302 ± 6 Ma (Table 4).

Three ore bodies consisting of gold-bearing veins and veinlets have been identified in various mylonites. The NE-trending ore bodies dip (70–85°) to the NW, range from 100 to 300 m in length, 0.5 to 2 m in thickness, and have downdip extent of 250 to 400 m. Mineralogical constituents of the gold ores and alteration zones at Houshihua are listed in Table 2.

Two stages of ore-forming processes are recognized: early and late stages. The early stage is represented by molybdenite–quartz veins varying from 0.8 to 2 m in thickness. The veins consist mainly of pyrite, molybdenite, chalcopyrite, quartz and sericite. Gold occurs as native gold, calaverite and petzite in microfractures of pyrite, molybdenite and quartz. The position of gold mineralized zone within the veins is variable, either in the core or close to the rim. Gold content up to 152 g/t is recorded. The late stage is represented by polymetallic sulfide–quartz disseminated-veinlets. These veinlets are mainly composed of chalcopyrite, pyrite, galena, sphalerite and quartz. Gold occurs mainly as native metal and calaverite. Both pyrite and quartz contain Au (10–95 g/t). Gold fineness is high (average 987), with only minor impurities of Ag (less than 0.6%), rare Cu, Fe and S. $^{40}Ar/^{39}Ar$ isotopic dating on sericite from the gold ores yields an age of 301 ± 5 Ma, which is similar to that of the mafic porphyry dyke (Table 4).

4.2. Gold deposits hosted by Proterozoic volcano-sedimentary rocks

4.2.1. Saiyinwusu, Darhan Muminggan Joint Banner

The Saiyinwusu deposit is located 126 km north of Baotou city (Fig. 1), and 10 km north of the Bayan Obo Fe–REE–Nb mine—the world's largest known REE deposit. The gold deposit was discovered in the early of 1980s by No. 11 Geological Party, Gold Headquarters, Ministry of Metallurgical Industry (MMI) during systematic geological mapping. It has
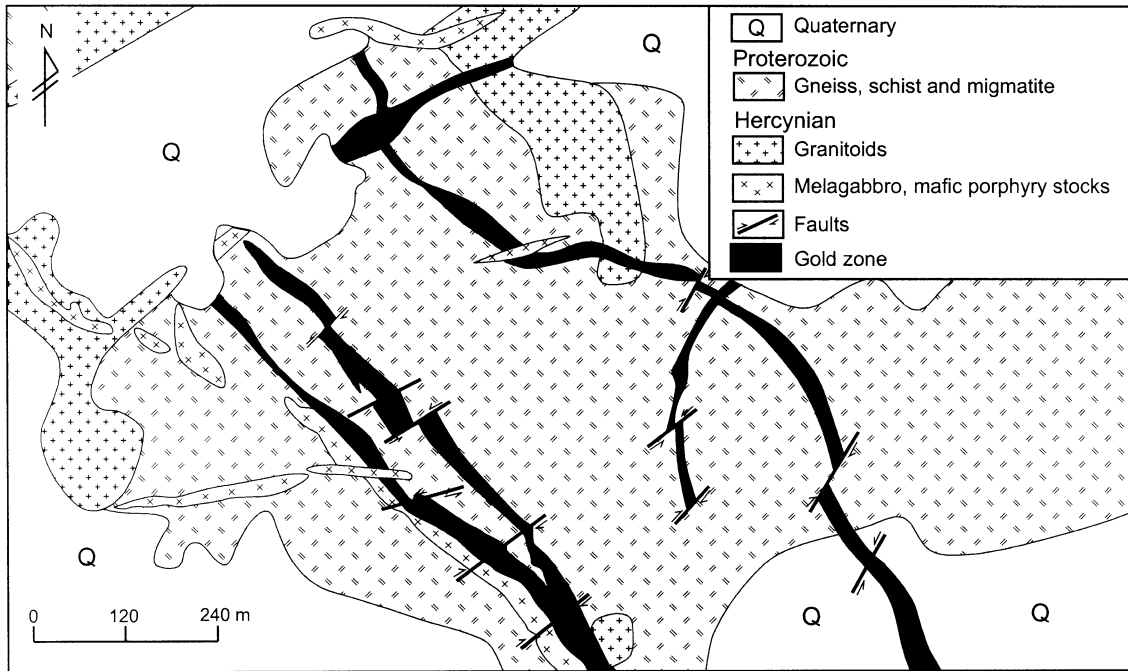
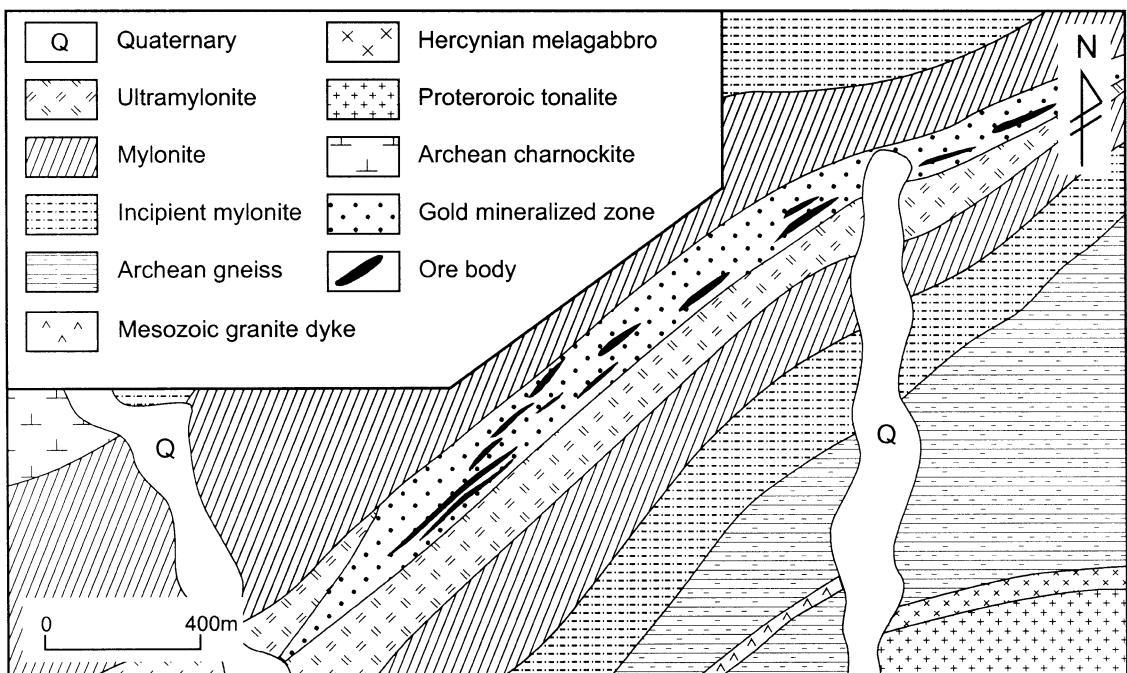Fig. 5. Schematic geological map of the Laoyanghao gold deposit.

Fig. 6. Schematic geological map of the Houshihua gold deposit.

a reserve of 12-t gold, with an average grade of 10 g/t gold. A local government mine started in the mid 1980s, and gold production commenced in 1988, with an annual production of 400 kg Au.

The Saiyinwusu deposit is tectonically situated in the western section of northern margin of the North China craton. The strata exposed in the district are mainly composed of Proterozoic quartzite, carbonate and shale of the Bayan Obo Group (Fig. 7). The geology in the Bayan Obo–Saiyinwusu area is described in detail in numerous publications (Institute of Geochemistry, 1988; Drew et al., 1990; Chao et al., 1992; Wang et al., 1992; Yuan et al., 1992; Gordon, 1993; Bai et al., 1996).

The host rocks for the gold deposit consist of crystalline limestone, quartzite, carbonaceous slate, iron-rich black slate, marl slate and sandstone of Halahuogete and Bilute Fms. (Y8 and Y9) of the Bayan Obo Group. It is noted that the host rocks are folded into a domal structure in the southern part of the district. The core of the dome consists of sandstone and siltstone, which are intensively faulted and fractured. Several NW-trending faults cut the domal core,

which hosts gold mineralization. These two formations are intruded by a numbers of Hercynian and Mesozoic Yanshanian mafic and granitoid stocks, dyke swarms and batholiths. No direct relationship between the gold ores and the Hercynian granitoid stocks, but disseminated gold mineralization occurring within the leucogabbro dykes or along their contacts with the Proterozoic sedimentary rocks, has been identified. The light-colored leucogabbro is composed mainly of fine- to medium-grained hornblende, plagioclase, clinopyroxene and biotite. $^{40}Ar/^{39}Ar$ isotopic age dating on hornblende from the leucogabbro dyke yields an age of 249 ± 5 Ma (Table 4).

Up to date, two mineralization zones have been outlined in the district: southern and northern zones, and are briefly described as follows.

4.2.1.1. Southern zone. Gold mineralization occurs in quartzite and siltstone, as veins, lenticular and disseminated-veinlets. Host rocks are strongly fractured and sheared, varying from brecciated rocks to mylonite. In this zone, nine ore bodies are delineated, of which Nos. 1, 2, and 5 are the largest ones, and
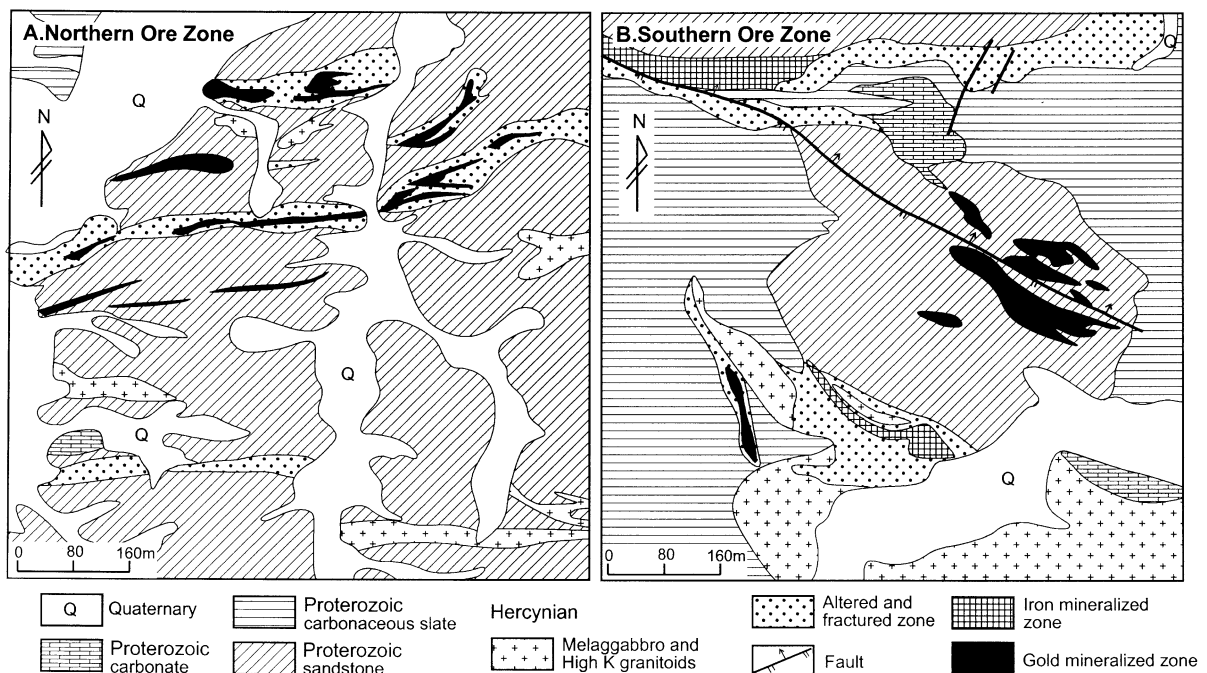

Fig. 7. Schematic geological map of the Saiyinwusu gold deposit.

constitute the major portion of this zone. These nine ore bodies mostly oriented in NW–SE direction vary in length from 3 to 250 m, and a thickness from 0.5 to 150 m. The down-dip extent of these ore bodies varies from 20 to 50 m. The mineralogy of primary gold ores is relatively simple, and is listed in Table 2.

A well-developed oxidized (supergene) ore zone has been observed in this zone. The oxidized ore zone varying from 50- to 70-m thick can be divided into lower and upper parts: (1) the lower part overlying the primary ore body has a thickness of 25 to 32 m. It consists mainly of limonite, goethite, jarosite, covellite, galena, arsenopyrite, native gold and native silver. The gangue mineral assemblage is microcline, quartz, sericite, kaolinite and illite; (2) the upper part has a thickness of 2 to 8 m. It is composed mainly of hematite, goethite, native gold, native silver, microcline, quartz, calcite, illite and kaolinite. In general, the oxidized zone contains about 4 to 18 g/t, Au and 3 to 16g/t Ag, and constitutes the important part of the ore body.

4.2.1.2. Northern zone. Gold mineralization occurs within Mesoproterozoic quartzite, and carbonaceous slate as single irregular veins, veinlet groups and en echelon lenses, which are mainly controlled by NE- and WE-trending fractures. These NE- and WE-trending gold veins dipping (38–59°) to the south and SE, range from 80 to 500 m in length, 0.5 to 8 m in width, and 200 to 450 m in decline depth. Generally, the gold ores with high gold content (>8 g/t) are distributed in the center of the gold-bearing quartz veins. The mineralogy of primary gold ores is similar as that of the Southern zone. $^{40}Ar/^{39}Ar$ isotopic dating on sericite separates from the gold ores gave an age of 249 ± 5 Ma, which is the same as that of the leucogabbro dyke associated with the ore bodies (Table 4). It is suggested that gold mineralization is essentially contemporaneous with emplacement of the leucogabbro dykes.

The development of hydrothermal alteration in both northern and southern zones depends on the size of the veins and the degree of fracturing of the host rocks. The simple quartz vein has a weak alteration with only a few decimeters to meters in thickness, but some complex veins are associated with intensive alteration. The most important alteration minerals observed in the Saiyinwusu deposits are listed in Table 2.

4.3. Gold deposits hosted by or related to Hercynian alkaline intrusions

As described above, Hercynian alkaline intrusive stocks and dyke swarms are widely distributed in the Baotou–Bayan Obo district. Some of these gold deposits and prospects are hosted by, or related to, aegirine–augite syenite and monzonite stocks and dyke swarms, among which the Wulashan and Donghuofeng deposits are largest ones. Both of these two deposits exhibit similarities to alkaline-type gold deposits described from elsewhere in the world, including the presence of alkaline igneous host rocks, intensive potassic alteration and gold-bearing tellurides (Mutschler et al., 1985; Bonham, 1988; Richards and Kerrich, 1993; Richards, 1995; Nie and Wu, 1998; Nie, 1998).

4.3.1. Wulashan deposit, Baotou
The Wulashan gold deposit is located about 20 km northwest of the Baotou city, and was discovered by No. 11 Geological Party, Gold Headquarters of Ministry of Metallurgical Industry. About 40 t of gold at grade of 5–30 g/t Au is identified. A local government gold mine was established in 1992. Crude ore production of the mine is 1000 t a day.

Hercynian alkaline syenite dykes and K-feldspar granite stocks are well developed, and intrude Archean gneiss–amphibolite–migmatite of the Wulashan Group (Fig. 8). All these alkaline intrusive dykes and stocks are WE-trending with north dip of 68° to 84° and thickness ranging from 1.5 to 7 m. Many dykes can be traced for more than 300 m along strike. Based on the field observations, three major intrusive phases have been recognized: (1) aegirine–augite syenite; (2) syenite porphyries; (3) nepheline syenite. Most of these syenite dykes consist mainly of K-feldspar (40–55 vol.%) and plagioclase (15–35 vol.%) with various amounts of aegirine–augite, nepheline and biotite. Accessory phases include magnetite, apatite, sphene, zircon and monazite. All these syenite dykes can be classified on the total alkali silica (TAS) diagram (Fig. 3) as trachy–dacite, and show a shoshonitic geochemical feature on the $K_2O\%$ vs. $SiO_2\%$ plot (Fig. 4). $^{40}Ar/^{39}Ar$ isotopic dating on K-feldspar separates from the alkaline syenite dykes have yielded two ages of 299 ± 3 and 298 ± 5 Ma, respectively (Table 4).
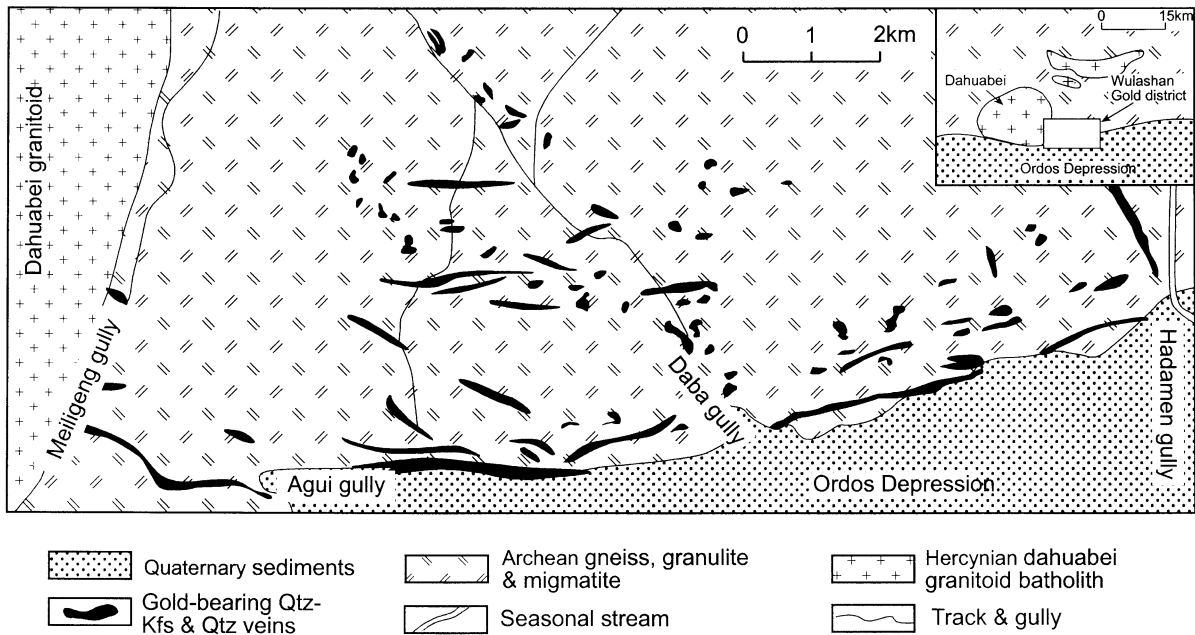
Fig. 8. Simplified geological map of the Wulashan gold deposit.

The gold mineralization occurs within the alkaline syenite dykes, and neighbouring Archean amphibolite, gneiss, leptynite and magnetite quartzite as irregular K-feldspar–quartz veins, stratoid layers and lenses, which are controlled by the WE- and NE-trending structures (Lang, 1990; Guo, 1992). The Hercynian syenite dyke swarms and stocks have been the targets of gold mineral exploration since the discovery of the Wula-shan deposit.

Based on geologic features and geographic locations, these gold-bearing veins can be divided into six vein groups. The No. 13 is the largest one, and contains about 70% of the total gold reserve of the Wulashan gold deposit. Located in the eastern part of the Wulashan gold district, the No. 13 vein is about 2200-m long and 3-m thick with declined depth of 500 m. The vein group generally occurs as roughly parallel veins, and associated auriferous fractured rocks. Ore mineralogy and alteration mineral assemblage of gold veins are relatively simple, and are listed in Table 2. Sericite separates from the gold ores have been dated by $^{40}Ar/^{39}Ar$ method at 297 ± 4 and 296 ± 4 Ma, respectively (Table 4). Clearly, the gold mineralization at Wulashan is essentially contempora-

neous with the emplacement of these Hercynian alkaline syenite dyke swarms.

The geological setting, geology, geochemistry, sulfur and lead isotopic features of the Wulashan gold deposit have already been described by Nie and Bjørlykke (1994).

4.3.2. Donghuofang deposit, Wuchuan

The Donghuofang deposit is located 20 km southwest of Wuchuan county (Fig. 9). It was discovered by geologists from Inner Mongolian Bureau of Geology and Mineral Resources in the mid 1980s during geological mapping (1:50 000). It has a reserve of 4 t of gold with an average grade of 5 g/t Au. Construction of a local government gold mine will be finished in the coming year, and is planned to produce 580 kg of Au annually.

The Donghuofang deposit is situated in the western section of the Inner Mongolian Axis within the North China craton. The strata exposed in the district comprise Archean biotite–hornblende–plagioclase gneiss, hypersthene–plagioclase gneiss, and marble. The entire sequence strikes NW and dips $70-85°$ NE. Minor folds and bedding-parallel faults occur. Three
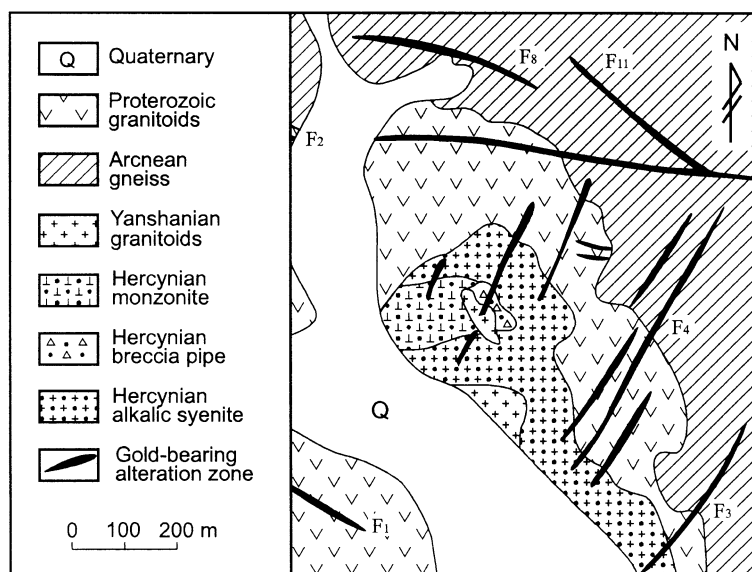
Fig. 9. Schematic geological map of the Donghuofang gold deposit.

major groups of fault and fracture zones are recognized within the mining district. A WE-trending subvertical fault, a group striking NE (20–32°), dipping either steeply (74°) or shallowly (20°) to the NW, and a group of subvertical faults striking NW and dipping to SW. The mineralized veins and alteration zones occur along all these three groups of faults and fractures.

Granitoid stock, dyke and batholith occur frequently in the district. The most important intrusion is the Donghuofang intrusive complex, which intrudes the Archean hyperthene–plagioclase gneiss. It has an outcrop of about 950-m long and 120- to 330-m wide. The intrusive complex is elongated NW–SE parallel to the regional strike of the wall rocks, and consists of monzonite, aegirine–augite syenite porphyry and a breccia pipe. Monzonite crops out in the central part of the intrusive complex, and is the earliest intrusive phase. It is an equigranular and halocrystalline rock consisting of quartz (0–5 vol.%), orthoclase (28–38%), plagioclase (40–50%), hornblende (2–8%) and magnetite, 0.5 to 2.5 mm in size. The monzonite has been dated by $^{40}Ar/^{39}Ar$ method at 280 ± 4 Ma (Table 4). Aegirine–augite syenite porphyry stock intrudes the diorite, and constitutes the northern and eastern portions of the intrusive complex. Orthoclase and aegirine–augite occur as phenocrysts, and albite, magnetite and aegirine–augite has also been seen in

the matrix. The syenite stock scatters over the field of trachy–andesite, and show shoshonitic geochemical feature (Figs. 3 and 4). Dating of two K-feldspar separates from this porphyry stock gives $^{40}Ar/^{39}Ar$ ages of 278 ± 4 and 276 ± 5 Ma, respectively. In the central part of the intrusive complex, a breccia pipe is recognized. The breccia has orthoclase, albite, and biotite, 1 to 3 mm in size as phenocrysts, and microcrystal aggregate of albite and orthoclase. Small amounts of biotite and glass are also found in its matrix. Xenoliths of diorite and syenite porphyry, 2 to 15 cm, sometimes 25 to 36 cm in size, have been observed in the breccia pipe.

The Donghuofang deposit consists mainly of gold-bearing K-feldspar–quartz veins and associated alteration zones, and occurs both within the intrusive complex and along the intrusive-wall rock contact. Five gold-bearing vein groups and associated alteration zones are delineated. The great concentration of veins and the richest mineralization occur in the intrusive complex. The gold mineralization occurs in single irregular veins, veinlet groups and en echelon lenses, which are mainly controlled by the NE- or WE-trending fractures. The gold-bearing K-feldspar–quartz vein varies from 60 to 540 m in length and 0.4 to 5 m in width, and has downdip extent of 300 to 450 m. The disseminated gold ores are developed within

the alteration zone around these major veins. In this type of ore, there is a continuous transition between economic ore bodies and the wall rocks. In general, the economic ore bodies are about 0.5- to 1.2-m thick, whereas the entire mineralized zone is commonly more than 3-m thick.

Mineralogical constituents of the gold ores, and altered and fractured rocks at Donghuofang, are listed in Table 2. $^{40}Ar/^{39}Ar$ isotopic dating on two sericite separates from the gold ores has yielded ages of 277 ± 4 and 276 ± 3 Ma (Table 4), respectively. The gold mineralization at Donghuofang is temporally related to the Hercynian alkaline magmatism.

5. Isotope studies

5.1. Sulfur isotopes

Sulfur isotope data for 78 pyrite, 19 galena and 2 pyrrhotite separates and 10 galena separates from six major gold deposits of the Baotou–Bayan Obo district are listed in Table 5 and plotted in Fig. 10. For these gold deposits hosted by Archean metamorphic rocks (type 1), the $\delta^{34}S$ values of 36 pyrite samples from Shibaqinhao, Laoyanghao and Houshihua vary from -4.0‰ to -0.1‰, with an average value of -2.3‰. No significant variation in the $\delta^{34}S$ values has been observed among the three gold deposits. Sulfur isotope data have also been obtained for pyrite, galena and pyrrhotite separates from the Saiyinwusu gold deposit hosted by Proterozoic sedimentary rocks (type 2). Twelve pyrite separates have $\delta^{34}S$ values varying from -2.4‰ to 2.3‰, and cluster between -2.4‰ and 1.0‰. Galena and pyrrhotite separates are relatively isotopically depleted. Six galena samples have $\delta^{34}S$ range of -3.1‰ to 0.9‰, with an average value of -1.3‰. No horizontal and vertical zonations of the sulfur isotope values are observed on these Precambrian metamorphic-hosted gold deposits (types 1 and 2).

For these gold deposits hosted by or related to Hercynian alkaline intrusive rocks, the $\delta^{34}S$ values of 12 pyrite separates from the Donghuofang gold deposit vary from -6.0‰ to -0.1‰, and cluster between -4.7‰ and -2.5‰. In contrast, the $\delta^{34}S$ values of pyrite and galena separates from the Wulashan gold deposit are relatively depleted. Twenty pyrite separates

have $\delta^{34}S$ values varying from -9.7‰ to -2.4‰, with an average value of -6.6‰. The $\delta^{34}S$ values of 13 galena separates from the gold-bearing quartz veins vary from -14.8‰ to -6.5‰, with an average value of -12.8‰, which is isotopically depleted. No horizontal zonation of the sulfur isotopic values is observed on both the Donghuofang and Wulashan gold deposits.

The $\delta^{34}S$ values of 12 magmatic pyrite samples from fresh Hercynian fresh monzonite and syenite intrusions range from 1.3‰ to 4.6‰, with an average value of 3.3‰. These compositions are much more enriched than those of sulfide separates from all six gold deposits in the Baotou–Bayan Obo district. In contrast, all those eight pyrite separates from Precambrian metamorphic rocks including gneiss, quartzite and slate have the most negative $\delta^{34}S$ values range of -20.2‰ to -15.8‰, with an average value of -17.7‰.

The Hercynian monzonite and syenite stocks (or dykes) in the vicinity of the gold occurrences in the district, yield pyrite separates that show positive $\delta^{34}S$ values ($1.3–4.6\text{‰}$), and are very similar to magmatic sulfide sulfur (Ohmoto and Rye, 1979). Moreover, the $\delta^{34}S$ values of two pyrite samples from a barren quartz vein cutting the syenite stock vary from 0.8‰ to 1.5‰. Theses values are compatible with sulfur of igneous origin. All these pyrite separates coming from Precambrian wall rocks of the gold occurrences are characterized by striking negative sulfur isotope values with a maximum of -20.2‰. Such depleted sulfur is characteristic of sulfide formed via bacterial reduction of sulfate under anoxic conditions in many submarine sedimentary environments (Ohmoto and Rye, 1979). It has also been noted that the $\delta^{34}S$ value of sulfide from the ore deposits falls in between the values of sulfides from the Hercynian alkaline intrusions and these of Precambrian metamorphic rocks. This intermediate $\delta^{34}S$ value range exhibits both magmatic and sedimentary characters.

The isotopic composition of sulfides from the Shibaqinhao, Laoyanghao, Houshihua, Saiyinwusu and Donghuofang gold deposits are within the $\delta^{34}S$ range of pyrites from many porphyry copper deposits ($-5.5–6.5\text{‰}$, Taylor, 1987). They are also typical for sulfide compositions in mesothermal gold deposits from many parts of the world (Lambert et al., 1984;

Table 5

Sulfur isotopic compositions of sulfides from major gold deposits in the Baotou−Bayan Obo district, Inner Mongolia, China

Sample No.	Mineral	δ^{34}S (‰)	Occurrence	Sample No.	Mineral	δ^{34}S (‰)	Occurrences
Shibaqinhao gold deposits hosted by Archean metamorphic rocks							
SBQ01	Py	− 2.6	Qtz vein	SBQ08	Py	− 3.3	Qtz vein
SBQ02	Py	− 2.4	Qtz vein	SBQ09	Py	− 2.8	Qtz vein
SBQ03	Py	− 1.8	Qtz vein	SBQ10	Py	− 3.1	Qtz vein
SBQ04	Py	− 0.1	Qtz vein	SBQ11	Py	− 1.8	Qtz vein
SBQ05	Py	− 3.0	Qtz vein	SBQ12	Py	− 2.9	Qtz vein
SBQ06	Py	− 1.3	Qtz vein	SBQ13	Py	− 2.8	Qtz vein
SBQ07	Py	− 2.6	Qtz vein	SBQ14	Py	− 1.9	Qtz vein
Laoyanghao gold deposits hosted by Archean metamorphic rocks							
LYH01	Py	− 0.1	Qtz vein	LYH06	Py	− 2.8	Qtz vein
LYH02	Py	− 1.8	Qtz vein	LYH07	Py	− 1.5	Qtz vein
LYH03	Py	− 3.5	Qtz vein	LYH08	Py	− 2.5	Qtz vein
LYH04	Py	− 1.5	Qtz vein	LYH09	Py	− 1.4	Qtz vein
LYH05	Py	− 0.8	Qtz vein	LYH10	Py	− 2.0	Qtz vein
Houshihua gold deposit hosted by Archean metamorphic rocks							
HSH01	Py	− 2.59	Qtz vein	HSH07	Py	− 3.21	Qtz vein
HSH02	Py	− 3.13	Qtz vein	HSH08	Py	− 2.76	Qtz vein
HSH03	Py	− 3.18	Qtz vein	HSH09	Py	− 2.21	Qtz vein
HSH04	Py	− 2.89	Qtz vein	HSH10	Py	− 4.01	Qtz vein
HSH05	Py	− 1.67	Qtz vein	HSH11	Py	− 2.61	Qtz vein
HSH06	Py	− 1.29	Qtz vein	HSH12	Py	− 2.35	Qtz vein
Saiyinwusu gold deposit hosted by Proterozoic sedimentary rocks							
SYW01	Gn	− 1.34	Qtz vein and veinlet	SYW10	Py	2.32	Qtz vein and veinlet
SYW02	Gn	− 2.42	Qtz vein and veinlet	SYW11	Py	− 2.12	Qtz vein and veinlet
SYW03	Gn	− 2.56	Qtz vein and veinlet	SYW12	Py	− 0.79	Qtz vein and veinlet
SYW04	Gn	0.46	Qtz vein and veinlet	SYW13	Py	− 1.89	Qtz vein and veinlet
SYW05	Gn	0.33	Qtz vein and veinlet	SYW14	Py	− 2.40	Qtz vein and veinlet
SYW06	Gn	− 3.01	Qtz vein and veinlet	SYW15	Py	0.89	Qtz vein and veinlet
SYW07	Py	− 2.04	Qtz vein and veinlet	SYW16	Py	0.77	Qtz vein and veinlet
SYW08	Py	− 0.66	Qtz vein and veinlet	SYW17	Po	− 3.03	Qtz veinlet
SYW09	Py	1.24	Qtz vein and veinlet	SYW18	Po	− 3.45	Qtz veinlet
Donghuofang gold deposit related to Hercynian alkaline intrusive rocks							
DHF01	Py	− 4.1	Qtz−Cc vein	DHF07	Py	− 2.8	Qtz−Kfs vein
DHF02	Py	− 6.0	Qtz−Cc vein	DHF08	Py	− 4.3	Qtz−Cc vein
DHF03	Py	− 0.1	Disseminated veinlet	DHF09	Py	− 3.8	Qtz−Cc vein
DHF04	Py	− 4.7	Qtz−Cc vein	DHF10	Py	− 1.8	Disseminated veinlet
DHF05	Py	− 3.2	Qtz−Kfs vein	DHF11	Py	− 1.5	Disseminated veinlet
DHF06	Py	− 3.6	Qtz−Kfs vein	DHF12	Py	− 2.5	Disseminated veinlet
Wulashan gold deposit related to Hercynian alkaline intrusive rocks							
W9020	Py	− 2.5	Qtz−Kfs vein	W9605	Py	− 5.1	Qtz−Kfs vein
W9021	Py	− 3.8	Qtz−Kfs vein	W9606	Py	− 4.8	Qtz−Kfs vein
W9022	Py	− 8.4	Qtz−Kfs vein	W9607	Py	− 8.4	Qtz−Kfs vein
W9023	Py	− 7.0	Qtz−Kfs vein	W9608	Py	− 3.2	Qtz vein
W9024	Gn	− 12.4	Qtz−Kfs vein	W9609	Py	− 8.2	Qtz vein
W9025	Gn	− 6.5	Qtz vein	W9610	Py	− 7.6	Qtz vein
W9026	Py	− 8.5	Qtz vein	W9611	Py	− 8.6	Qtz vein
W9027	Gn	− 13.5	Qtz vein	W9612	Gn	− 14.6	Qtz vein
W9028	Py	− 8.2	Qtz vein	W9613	Gn	− 13.2	Qtz vein

Table 5 (continued)

Sample No.	Mineral	$\delta^{34}S$ (‰)	Occurrence	Sample No.	Mineral	$\delta^{34}S$ (‰)	Occurrences
Wulashan gold deposit related to Hercynian alkaline intrusive rocks							
W9029	Py	− 9.7	Qtz vein	W9614	Gn	− 13.6	Qtz vein
W9030	Gn	− 12.3	Qtz vein	W9615	Gn	− 14.8	Qtz vein
W9031	Py	− 7.5	Qtz vein	W9616	Gn	− 14.6	Qtz vein
W9032	Py	− 8.4	Qtz vein	W9617	Gn	− 14.4	Qtz vein
W9601	Py	− 2.4	Qtz vein	W9618	Gn	− 14.1	Qtz vein
W9602	Py	− 7.9	Qtz−Kfs vein	W9619	Gn	− 13.7	Qtz vein
W9603	Py	− 4.6	Qtz−Kfs vein	W9620	Gn	− 8.8	Qtz vein
W9604	Py	− 7.4	Qtz−Kfs vein				
Hercynian alkaline intrusions and related Qtz vein							
W9045	Py	2.6	Cpx−Hbl monzonite stock	W9627	Py	2.8	WLS syenite dyke
W9046	Py	4.1	Cpx−Hbl monzonite stock	W9628	Py	3.4	DHF syenite stock
W9056	Py	1.3	Cpx−Hbl monzonite stock	W9629	Py	2.8	DHF syenite stock
W9057	Py	2.0	Cpx−Hbl monzonite dyke	W9630	Py	4.3	DHF syenite stock
W9624	Py	4.6	WLS syenite stock	W9631	Py	4.8	DHF syenite stock
W9625	Py	3.7	WLS syenite stock	W9632	Py	0.76	Qtz vein
W9626	Py	3.6	WLS syenite dyke	W9633	Py	1.45	Qtz vein
Precambrian metamorphic rocks							
W9052	Py	− 17.0	Archean Sill−Bt gneiss	W9622	Py	− 17.9	Archean quartzite
W9054	Py	− 18.3	Archean Sill−Bt gneiss	W9623	Py	− 20.2	Archean quartzite
W9055	Py	− 18.5	Archean Hbl−Pl gneiss	W9624	Py	− 16.2	Proterozoic slate
W9621	Py	− 17.4	Archean Hbl−Pl gneiss	W9625	Py	− 15.8	Proterozoic slate

The sulfur isotope analyses were performed at the Institute of Mineral Deposits, Chinese Academy of Geological Sciences. Analytical procedures were described in the text.

Abbreviations: Bt = biotite; Cc = calcite; Cpx = clinopyroxene; DHF = Donghuofang; Gn = galena; Hbl = Hornblende; Kfs = K-feldspar; Pl = plagioclase; Py = pyrite; Qtz = quartz; Sill = sillimanite; WLS = Wulashan.

Data of W9020−W9032, W9045−W9057 and W9052−W9055 are from Nie and Bjørlykke (1994).

Kerrich, 1987; Peters and Golding, 1987; Groves and Foster, 1991; Trumbull et al., 1992). According to Ohmoto and Rye (1979) and Ohmoto (1986), such $\delta^{34}S$ values are consistent with a deep-seated source of sulfur either from leaching of metamorphic rocks or from igneous intrusions. In addition, the isotopic composition of sulfide minerals depends also on the chemistry of solution from which they crystallized. Therefore, the author cannot rule out the possibilities that such sulfur isotopic values result from a change in oxygen fugacity or mixing of fluids. The intermediate $\delta^{34}S$ value range of sulfides from the gold deposits suggests that sulfur was partially derived from the alkalic magma and Precambrian metamorphic rocks.

The sulfur isotope data of pyrite and galena samples from the Wulashan gold deposits (type 3) are obviously different from other mesothermal gold districts (Table 5), both in their variability and depleted values. Sulfides from most of these mesothermal gold deposits, including Archean deposits and those of the California Mother Lode, have $\delta^{34}S$ values of − 0.5‰ to 3.5‰ (Taylor, 1987; Bohlke et al., 1988). Those with $\delta^{34}S$ values more negative than − 3‰ are variably accompanied by hypogene sulfate minerals (Goldfarb et al., 1991). Phillips et al. (1986) found that high negative $\delta^{34}S$ values for pyrite samples from the gold-bearing quartz veins occur under relatively oxidizing conditions. However, many pyrites with depleted sulfur isotope values from the Shibaqinhao, Laoyanghao, Houshihua, Saiyinwusu, Donghuofang and Wulashan deposits are accompanied by fine-grained pyrrhotite or arsenopyrite. No sulfate minerals have been identified in the six gold deposits and their wall rocks. Similar sulfur isotope signatures for sulfides are also reported for the Dongping alkalic-type gold deposit (Nie, 1998). The absence of sulfate minerals at the gold occurrences of the Baotou−Bayan Obo district is char-
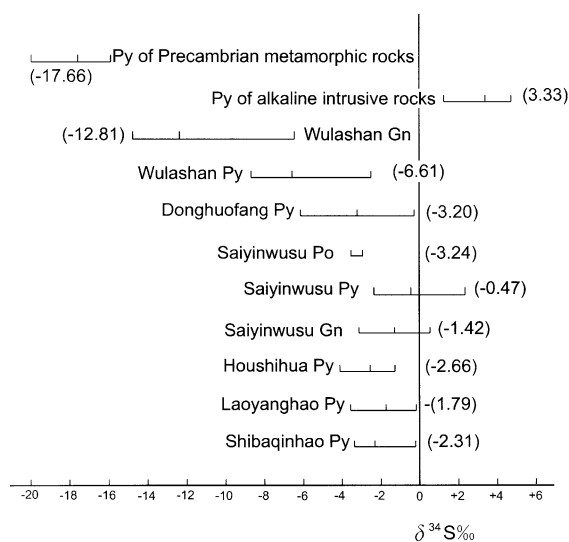
Fig. 10. Comparison of sulfide sulfur isotope data for the gold ores, Hercynian alkaline intrusions and Archean metamorphic wall rocks from major gold deposits in the Baotou–Bayan Obo district.

acteristic of Mesozoic mesothermal vein deposits (Taylor, 1987). Since pyrite will have a slightly higher $\delta^{34}S$ value (about 1 ‰) than H_2S in the fluid at 300 to 400 °C (Ohmoto and Rye, 1979), and the gold ores were formed under a reducing environment, the sulfur species in the fluid would have been predominantly H_2S and HS^-. Consequently, the measured $\delta^{34}S$ values of pyrite could represent the $\delta^{34}S$ value of the total sulfur in the fluids.

There are three ways to explain the variation in sulfur isotopic characteristics observed in the six gold deposits of the Baotou–Bayan Obo district. The first is that the variation resulted from a shifting oxidation state in the mineralizing fluids. The sulfides will gradually become isotopically depleted as the fluid is oxidized (Ohmoto, 1986). The second possibility is mixing of fluids with different isotopic composition. The third and preferred possibility is that magmatic fluids interacted with isotopically depleted wall rocks. Inasmuch as the gold mineralization at the six gold deposits described above is spatially and temporally associated with Hercynian alkaline intrusions, and occurs within Precambrian metamorphic rocks, it seems likely that sulfur in these six gold occurrences could have resulted from mixing of Hercynian alkaline magma and Precambrian metamorphic rocks. Interaction of alkaline magmatic fluid and Precam-

brian gneiss, quartzite and slate, including some carbonaceous materials (graphite), may result in a strong depletion of ^{34}S in the ore fluid (Goldfarb et al., 1991) and in sulfides with negative $\delta^{34}S$ values.

5.2. Lead isotopes

Lead isotope data of 19 pyrite separates from the Shibaqinhao, Laoyanghao, Houshihua, Saiyinwusu and Donghuofang gold deposits are listed in Table 6. They are also plotted in $^{207}Pb/^{204}Pb$ vs. $^{206}Pb/^{204}Pb$ and $^{208}Pb/^{204}Pb$ vs. $^{206}Pb/^{204}Pb$ diagrams (Figs. 11 and 12), together with the growth curves of Zartman and Haines (1988). For comparison, lead isotope data of four Hercynian alkaline intrusive and three Archean amphibolite whole rock samples as well as sulfide lead isotopic field of the Wulashan deposit (Nie and Bjørlykke, 1994) are also plotted in Figs. 11 and 12. All of these pyrite separates from these gold deposits in the Baotou–Bayan Obo district have a large spread in $^{206}Pb/^{204}Pb$ ranging from 16.8245 to 18.7491; relatively high $^{207}Pb/^{204}Pb$ ratios from 15.3767 to 15.6034 and $^{208}Pb/^{204}Pb$ from 36.7430 to 37.8801 (Figs. 11 and 12). Based on Doe and Stacey (1974), the calculation of Pb isotopic data shows that the single-stage model ages of these pyrite separates vary from −92 to 955 Ma (Table 6). Although most of these age data are geologically meaningless, some of the pyrite samples, with Pb single-stage age over 600 Ma, may imply that Precambrian materials were involved during their crystallization. Three Archean amphibolite whole rock samples have relatively low $^{206}Pb/^{204}Pb$ ratios, ranging from 16.1532 to 16.7146; narrow $^{207}Pb/^{204}Pb$ ratios, from 15.2601 to 15.3230 and $^{208}Pb/^{204}Pb$ from 36.0146 to 36.1678. Their Pb single-stage model age varies from 929 to 1317 Ma, which is geologically meaningless. All of these four syenite whole rock samples have relatively high $^{206}Pb/^{204}Pb$ ratio ranging from 18.7032 to 19.0836; $^{207}Pb/^{204}Pb$ from 15.6206 to 15.6884 and $^{208}Pb/^{204}Pb$ from 38.0432 to 38.8320. They contain more radiogenic lead than that of Archean amphibolite and sulfides from the gold deposits. On the $^{207}Pb/^{204}Pb$ vs. $^{206}Pb/^{204}Pb$ diagram (Fig. 11), these lead isotope data for the sulfides from the gold deposits, Archean amphibolite and Hercynian syenite whole rock samples cluster in three main fields. It has been noted that most data for the sulfides from the gold deposits plot

Table 6

Lead isotope compositions of pyrite separates from the major gold deposits and their wall rocks in the Baotou–Bayan Obo Area, Inner Mongolia, China

Sample No.	Order No.[a]	Occurrence	Material[b]	$^{206}Pb/^{204}Pb$	$^{207}Pb/^{204}Pb$	$^{208}Pb/^{204}Pb$	Model age (Ma)[c]	μ[c]
Gold deposits hosted by Archean high-grade metamorphic rocks								
(1) Shibaqinhao gold deposit								
SBQ01	1	Gold-bearing Qtz vein	Py	17.7413	15.4834	37.0843	432	9.335
SBQ02	2	Gold-bearing Qtz vein	Py	17.6352	15.4362	37.2087	417	9.152
SBQ03	3	Gold-bearing Qtz vein	Py	17.3867	15.4370	37.3341	616	9.237
SBQ04	4	Gold-bearing Qtz vein	Py	17.5004	15.4031	37.0540	455	9.042
(2) Laoyanghao gold deposit								
LYH01	5	Gold-bearing Qtz vein	Py	17.0067	15.3767	37.1042	798	9.–98
LYH02	6	Gold-bearing Qtz vein	Py	17.2034	15.4278	36.8346	742	9.264
LYH03	7	Gold-bearing Qtz veinlet	Py	17.0896	15.4417	36.8895	868	9.409
LYH04	8	Gold-bearing Qtz veinlet.	Py	16.8245	15.3824	36.7430	955	9.214
(3) Huoshihua gold deposit								
HSH01	9	Gold-bearing Qtz vein	Py	17.4986	15.4836	37.3047	622	9.416
HSH02	10	Gold-bearing Qtz vein	Py	17.4732	15.5012	37.1467	676	9.509
HSH03	11	Gold-bearing Qtz vein	Py	17.3245	15.4674	37.0832	725	9.405
Gold deposits hosted by Proterozoic meta-sedimentary rocks								
(4) Saiyiwusu gold deposit								
SYW01	12	Gold-bearing Qtz-Ser rock	Py	17.7535	15.5306	37.5804	519	9.547
SYW02	13	Gold-bearing Qtz veinlet	Py	17.8837	15.5267	37.3876	411	9.489
SYW03	14	Gold-bearing Qtz veinlet	Py	18.0736	15.5502	37.5808	314	9.542
Gold deposits hosted by or related to Hercynian alkaline intrusions								
(5) Donghuofang gold deposit								
DHF01	15	Gold-bearing Kfs–Qtz vein	Py	18.0735	15.5230	37.6826	256	9.421
DHF02	16	Gold-bearing Kfs–Qtz vein	Py	18.3842	15.5296	37.8329	27	9.379
DHF03	17	Gold-bearing Kfs–Qtz vein	Py	18.3812	15.5735	37.6868	127	9.569
DHF04	18	Gold-bearing Kfs–Ser rock	Py	18.2530	15.5506	37.6344	176	9.499
DHF05	19	Gold-bearing Kfs–Ser rock	Py	18.7491	15.6034	37.8801	– 92	9.623
Hercynian alkaline intrusions								
AN9901	20	Alkaline syenite stock	WR	18.7032	15.6206	38.0864	– 18	9.705
AN9902	21	Alkaline syenite stock	WR	19.0623	15.6212	37.8320	– 295	9.646
AN9903	22	Alkaline syenite dyke	WR	18.8804	15.6482	38.0432	– 92	9.789
AN9904	23	Alkaline syenite dyke	WR	19.0836	15.6884	38.1969	– 157	9.922
Archean metamorphic rocks								
MR9901	24	Archean amphibolite	WR	16.1532	15.2846	36.0146	1317	9.116
MR9902	25	Archean amphibolite	WR	16.2589	15.2601	35.7530	1184	8.903
MR9903	26	Archean amphibolite	WR	16.7146	15.3230	36.1678	929	8.968

Abbreviations: Kfs = K-feldspar; Py = pyrite; Qtz = quartz; Ser = serite; WR = whole rock.

[a] Order No.—numbers corresponding to that of Figs. 11 and 12.

[b] Material—mineral or whole rock samples.

[c] Model age (Ma) and μ—calculated Based on these parameters provided by Doe and Stacey (1974).

in between the Hercynian alkaline syenite and Archean amphibolite fields. As a whole, all these lead isotope data are roughly co-linear. They define a mixing line with a slope of 0.1338 ± 0.0003 (2σ), and an upper intersection age of $– 80$ Ma and a lower intersection age at 2183 Ma with the growth curve (Stacey and Kramers, 1975). Both these two ages are younger than that of the gold deposits and the Archean amphibolite, respectively. The data may indicate that the U–Th–Pb systems of the Archean amphibolite, Hercynian alkaline syenite and gold deposits have been strongly disturbed during the late geological events.
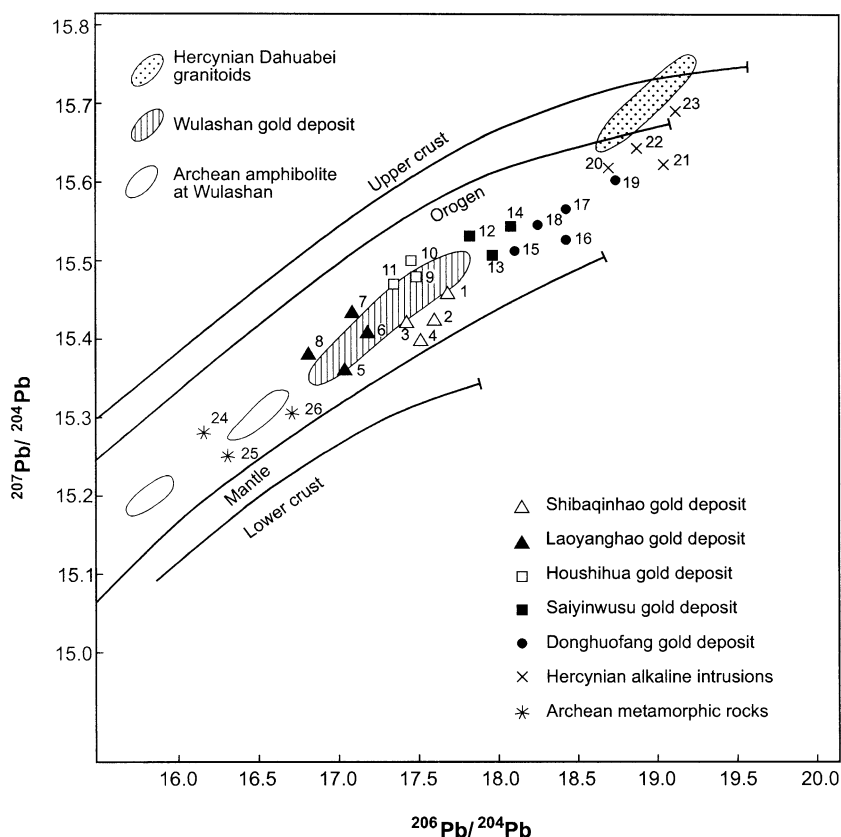
Fig. 11. $^{207}Pb/^{204}Pb$ vs. $^{206}Pb/^{204}Pb$ diagram of pyrite separates from the gold ores and whole rock samples of Archean amphibolite and Hercynian alkaline intrusions at Shibaqinhao, Laoyanghao, Saiyinwusu and Donghuofang. Also shown for comparison are fields of the gold ore, associated Hercynian high K intrusion and Archean metamorphic wall rocks of the Wulashan gold deposit (Nie and BjØrlykke, 1994). Pb isotope curves for the upper crust, lower crust, orogen and mantle are from Zartman and Haines (1988).

Although the fields of lead isotopic compositions of the pyrite separates from all these six gold deposits of the Baotou–Bayan Obo district overlap (Fig. 11), the obvious shift is observed to be systematic from Laoyanghao through Shibaqinhao and Houshihua to Donghuofang and Saiyinwusu. The most radiogenic pyrite come from the Donghuofang gold deposit hosted by or related to Hercynian alkaline intrusions. The trend toward higher $^{207}Pb/^{204}Pb$ for these pyrite separates suggests that mineralizing fluids may contain lead derived from a source with a relatively high U/Pb ratio. The high $^{206}Pb/^{204}Pb$, $^{207}Pb/^{204}Pb$ and $^{208}Pb/^{204}Pb$ ratios in the Hercynian alkaline syenites may reflect a high content of radiogenic Pb in the magmatic hydrothermal ore-forming solution. Contamination of the ore fluid could, therefore, in the case

of the gold deposits in the Baotou–Bayan Obo district, resulted in a significant depletion in the radiogenic lead isotope composition. It could be the result of the interaction between the ore fluid and supracrustal sequences and/or by mixing magmatic and meteoric fluids. Inasmuch as the gold deposits of the Baotou–Bayan Obo district are temporally associated with the Hercynian alkaline intrusions, and occur in Precambrian metamorphic rocks, it is reasonable to suggest that Hercynian alkaline magma contributed radiogenic Pb component to the ore fluids at the time of the formation of the deposit. This hypothesis is also supported by the sulfur isotope data described above.

The lead isotope composition of the sulfide minerals from the Shibaqinhao, Laoyanghao, Houshihua, Saiyinwusu, Wulashan and Donghuofang deposits
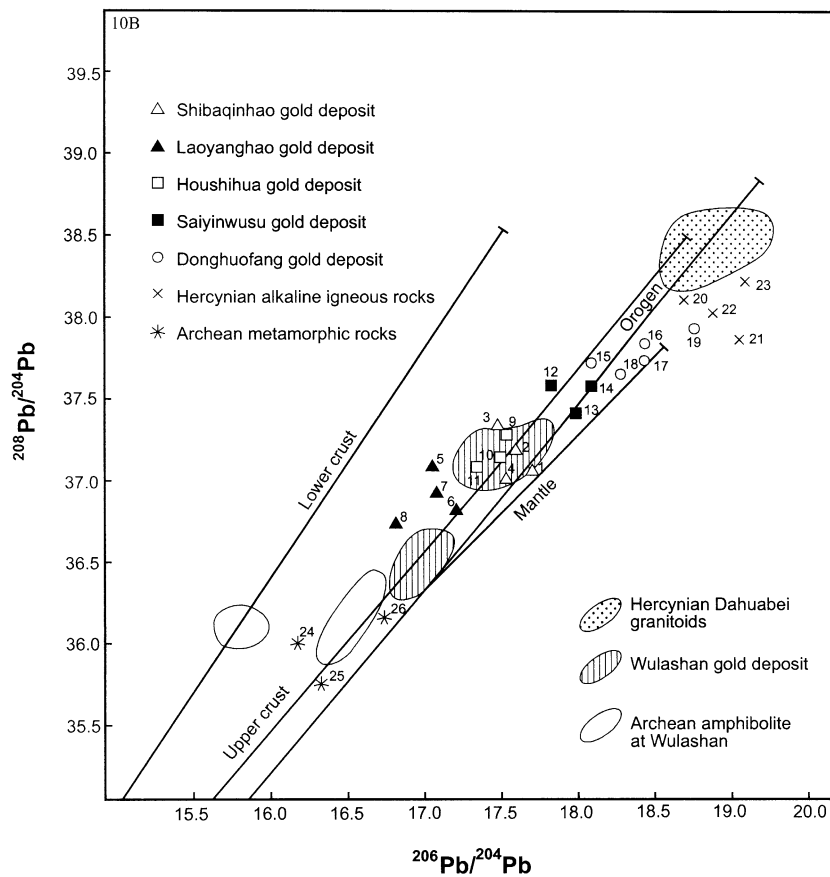
Fig. 12. $^{208}Pb/^{204}Pb$ vs. $^{206}Pb/^{204}Pb$ diagram of pyrite separates from the gold ores and whole rock samples of Archean amphibolite and Hercynian alkaline intrusions at Shibaqinhao, Laoyanghao, Saiyinwusu and Donghuofang. Also shown for comparison are fields of the gold ore, associated Hercynian high K intrusion and Archean metamorphic wall rocks of the Wulashan gold deposit (Nie and Bjørlykke, 1994). Pb isotope curves for the upper crust, lower crust, orogen and mantle are from Zartman and Haines (1988).

reflects the dominant gold mineralization in the Baotou–Bayan Obo district. Most of the pyrite samples from these gold occurrences plot about halfway between the Hercynian alkaline intrusions and Archean amphibolite (Figs. 11 and 12). Similar Pb-isotope signatures spread out between values of Phanerozoic intrusions and surrounding Precambrian metamorphic rocks have been reported for other gold deposits around the North China craton (Lin and Guo, 1985; Wang et al., 1990; Trumbull et al., 1992; Nie and Bjørlykke, 1994; Nie, 1998; Nie et al., 2000). These data suggest that mixing of Pb from two distinct reservoirs is a consistent characteristic of the Hercynian igneous belt of gold ores.

Significant scatter in the $^{208}Pb/^{204}Pb$ ratios for the gold deposits reflects a variable U/Th ratio in the source (Fig. 12). An input of radiogenic lead-bearing material or fluids to the initial Pb-isotope system is possible during the ore-forming processes. Although the source of lead in the deposit need not be the same as the source of gold, there is a paragenetic association between gold and pyrite in the ores, especially the Wulashan and Donghuofang deposits. This may indicate that both pyrite and gold mineral were precipitated from the same ore-forming fluids.

6. Discussion and conclusions

Hercynian tectonism, causing widespread faulting, fracturing and alkaline magmatism, is the most important event for the formation of the gold deposits in the

Baotou–Bayan Obo district, Inner Mongolia. Most of these deposits are located within or near the Chaertai and Bayan Obo paleorifts that formed around 1500 Ma (Wang et al., 1992; Bai et al., 1996). The Chuanjing–Bulutai deep-seated fault marks the closing of the ancient Mongolian ocean between the Angara and North China craton (Wang and Liu, 1991) (Fig. 1). The ultimate cause of the alkalic magmatism in the Baotou–Bayan Obo district is thought to be an extensional event perhaps due to the reworking of the Chaertai and Bayan Obo paleorifts. Such a tectonic environment is favorable for the generation and emplacement of mantle-derived alkaline magmas and associated gold mineralization (Kelley et al., 1996; Nie and Wu, 1998; Nie, 1998).

Deep-seated faulting and fracturing derived by W–E compression and N–S tensile stress in the Baotou–Bayan Obo district initiated mafic magmatism, resulting in widespread diabase and gabbro dykes. These mafic intrusions are followed by subsequent alkaline magmatism and gold mineralization. Zhang (1991) indicate that all these alkaline syenite and monzonite stocks and dykes are derived sequentially from similar magma chambers situated under the Chaertai and Bayan Obo paleorifts and their surrounding areas.

Mineralogical and textural observations of these gold-bearing alkaline syenite and monzonite stocks (or dykes) suggest that the parental magma was volatile rich (CO_2, H_2O, and Cl) and moderately oxidized (Nie and Wu, 1998). During its ascent, the alkaline magma underwent degassing, and was contaminated with Archean metamorphic and Proterozoic sedimentary rocks. Meanwhile, an input of heat by the emplacement of these alkaline intrusions caused hydrothermal circulation and steepened geothermal gradients. As a result, the higher level of the magma chamber is rich in volatiles such as H_2O, S, and CO_2, precious metals, K_2O and Na_2O. A large volume of fluid was evolved from the melt as evidenced by the large amount of veining within these alkaline intrusive dykes.

Mineralogical, geochemical and isotopic studies indicate that both Wulashan and Donghuofang gold deposits (type 3) were formed by magmatic–hydrothermal fluid. The fluid that was mainly exsolved from the Hercynian alkaline magma was of high temperature (270–320 °C), with relatively high salinity ranging from 7 to 18 wt.% NaCl equivalent.

Sulfur and lead isotopic data suggest that a certain amount of ore-forming material derived from wall rocks was involved in the formation of these two gold deposits.

Most of these gold-bearing quartz veins or veinlet groups at Shibaqinhao, Laoyanghao, Houshihua and Saiyinwusu (types 1 and 2) are surrounded by an alteration halo dominated by quartz, sericite, chlorite, epidote and pyrite. Lower fluid temperatures (200–230 °C) and salinities (3 to 8 wt.% NaCl equivalent) are recorded from the fluid inclusions in these veins, and are indicative of differences in fluid temperature and composition compared to type 3 deposits. It seems likely that the ore-forming materials of the types 1 and 2 deposits could have resulted from mixing of Hercynian alkaline magma and Precambrian metamorphic wall rocks. The evolved meteoric water may also be involved in the formation of these Precambrian metamorphic-hosted gold deposits. Oxygen, hydrogen, carbon (Zhang, 1991; Nie et al., 2000) and sulfur isotope data suggest that the magma-derived heat, volatile (H_2O, S and C), and perhaps metals were added to the evolved meteoric hydrothermal fluids. The ore fluids were localized by active faults that were eventually sealed by quartz veins or veinlets. Most of the alteration-, ore- and vein-forming constituents as illustrated by the lead isotope data, were probably also redistributed from the alkaline intrusion and Precambrian metamorphic rocks. Although the oxygen, hydrogen, carbon and sulfur isotope data support the involvement of evolved meteoric water in the mineralizing system, they also allow for a direct alkaline magmatic contribution of fluids and metals. It is important to note that the alkaline intrusions that drove the ore-forming hydrothermal fluids were probably formed around 299 Ma (Late Carboniferous). The relative position of Late Carboniferous paleosurface with respect to the present erosional surface is thus a critical factor in the interpretation of these gold deposits in the Baotou–Bayan Obo district. Contributions from buried intrusions other than those presently exposed cannot be discounted.

The role of Precambrian basement in the formation of the gold deposits (types 1 and 2) is still problematic. The presence of basement rocks is a useful first-order parameter for the location of these gold deposits in the Baotou–Bayan Obo district. It can be best

explained by the evidences that faults and fractures occurring within the basement were generated in conjunction with the emplacement of large volumes of Hercynian alkaline magma during Hercynian orogeny. Clearly, the basement rocks have contributed some metallic components via their interaction with circulating evolved meteoric hydrothermal fluids. Since these deposits occur within a wide variety of basement lithologies, it seems unlikely that the nature of the Precambrian basement is critical for the localization of the gold ores.

Acknowledgements

References

Bai, G., Yuan, Z.X., Wu, C.Y., Zhang, Z.Q., Zheng, L.X., 1996. Demonstration on the Geological Features and Genesis of the Bayan Obo Ore District. Geological Publishing House, Beijing, pp. 1–104, in Chinese with English abstract.

Birkeland, A., 1990. Pb-isotope analysis of sulfides and K feldspars: a short introduction to analytical techniques and evolution of results: Mineralogisk Museum, University of Oslo, Internal Skriftserie 15, 32 pp.

Bohlke, J.K., Coveney Jr., R.M., Rye, R.O., Barnes, I., 1988. Stable isotope investigations of gold quartz veins at the Oriental mine, Alleghany district, California. US Geological Survey Open-File Report 88-279, 24 pp.

Bonham, H.F., 1988. Models for volcanic-hosted epithermal precious metal deposits. In: Schafter, R.W., Cooper, J.J., Vikre, P.G. (Eds.), Bulk Mineable Precious Metal Deposits of the Western United States. Symposium Proceedings. Reno. Geol. Soc., Nevada, pp. 259–271.

Bureau of Geology and Mineral Resources of Inner Mongolia, 1991. Regional geology of Nei Mongol (Inner Mongolia) Autonomous Region. Geological Publishing House, Beijing, pp. 630–651 (in Chinese).

Chao, E.T.C., Back, J.M., Minkin, J.A., Ren, Y., 1992. Host-rock controlled epigenetic hydrothermal metasomatic origin of the Bayan Obo REE–Fe–Nb deposit, Inner Mongolia, PRC. Appl. Geochem. 7, 443–458.

Chen, J.M., Liu, G., Li, C.C., Shi, Z.L., Zhang, L.Q., Wang, X.H., 1996. Geology of greenstone-type gold deposits in the Wula-Daqing Mt., Inner Mongolia, China Geological Publishing House, Beijing 165 pp. (in Chinese with English abstract).

Conrad, J.E., Mckee, E.H., 1992. ^{40}Ar/^{39}Ar dating of vein amphibole from the Bayan Obo iron–rare earth element–niobium deposit, Inner Mongolia, China: constraints on mineralization and deposition of the Bayan Obo group. Econ. Geol. 87, 185–188.

Davis, G.A., Wang, C., Zheng, Y., Zhang, J., Zhang, C., Gehrels, G.E., 1998. The enigmatic Yinshan fold and thrust belt of northern China: new views on its intraplate contractional styles. Geology 26, 43–46.

Doe, B.R., Stacey, J.S., 1974. The application of lead isotopes to the problems of ore genesis and ore prospect evaluation: a review. Econ. Geol. 69, 757–776.

Drew, L.J., Meng, Q.R., Sun, W.J., 1990. The Bayan Obo iron–rare–earth–niobium deposit, Inner Mongolia, China. Lithos 26, 43–65.

Gan, S.F., Qiu, Y.M., Yang, H.Y., Van Reenen, D.D., 1994. The Hadamengou mine—a typical gold deposit in the Archean granulite facies terrane of the North China craton. Int. Geol. Rev. 36, 850–866.

Geological Institute of Inner Mongolia, 1988, The application of integrated synthesis on exploration of gold deposits in central Inner Mongolia. Research Report. Huhhot, Bureau Geol. Mineral Resour., Inner Mongolia, 245 pp., in Chinese.

Geological Institute of Inner Mongolia, 1990. Geological and geophysical maps (1:200,000) of Central Inner Mongolia. Huhhot, Bureau Geol., Mineral Resour., Inner Mongolia, unpublished map, in Chinese.

Goldfarb, R.J., Newberry, R.J., Pickthorn, W.J., Gent, C.A., 1991. Oxygen, hydrogen, and sulfur isotope studies in the Juneau gold belt, southeastern Alaska: constraints on the origin of hydrothermal fluids. Econ. Geol. 86, 66–80.

Gordon, A.G., 1993. Rare earth elements and niobium in iron formation at Bayan Obo, Inner Mongolia, China. In: Maurice, Y.T. (Ed.), Proceedings of the Eighth Quadrennial IAGOD Symposium, Stuttgart, pp. 53–73.

Groves, D.I., Foster, R.P., 1991. Archean lode gold deposits. In: Foster, R.P. (Ed.), Gold Metallogeny and Exploration. Blackie, Glasgow, pp. 63–103.

Guan, L.X., 1993. Ore-forming process of the Wulashan gold deposit, Inner Mongolia. J. Gold Geosci. Technol. 3, 1–5, in Chinese.

Guo, Y.T., 1992. The minerogenetic geology of Hadamengou type gold deposits in Wulashan, Inner Mongolia. J. Precious Met. Geol. 1, 191–195, in Chinese.

Guo, Y.T., Wu, L.X., 1989. Geologic features and mineral exploration of the Wulashan gold deposit. J. Gold Geosci. Technol. 4, 27–33, in Chinese.

Hu, B.Q., Chang, Y.Z., Zhang, W.C., 1990. Characteristics of a large-scale nappe structure of the Yanshan–Yinshan mountain (Baotou district) and its relation to regional metallogeny of gold mineralization. J. Inner Mong. Geol. 1, 1–7, in Chinese.

Institute of Geochemistry of the Chinese Academy of Sciences, 1988. Geochemistry of Bayan Obo Deposit. Science Press, Beijing, pp. 65–99, in Chinese.

Jahn, B.M., Auvray, B., Cornichet, J., Bai, Y.L., Shen, Q.H., Liu, D.Y., 1987. 3.5-Ga old amphibolites from eastern Hebei province, China: field occurrence, petrography, Sm–Nd isochron age and REE geochemistry. Precamb. Res. 34, 311–346.

Jia, W.G., Chen, S.W., Han, Z.W., 1999. Large-scale metallogenic prognosis of the Donghuofang gold deposit. J. Precious Met. Geol. 8 (3), 155–162.

Kelley, K.D., Romberger, S.B., Beaty, D.W., Snee, L.W., Stein, H.J., Thompson, R.B., 1996. Genetic model for the Cripple Creek district: constraints from ^{40}Ar/^{39}Ar geochronology, major and trace element geochemistry, and stable and radiogenic isotope data. In: Thompson, T.B. (Ed.), Dimonds to Gold: I. State mine, Kimberlite district, Colorado. Soc. Econ. Geol. Guidebook Ser., 26. Economic Geology Publishing Company, El Paso, Texas, pp. 65–83.

Kerrich, R., 1987. The stable isotope geochemistry of Au–Ag vein deposits in metamorphic rocks. Mineral. Assoc. Canada, Short Course Handbook, vol. 13. Geological Survey of Canada, Ottawa, pp. 287–336.

Lambert, I.B., Phillips, G.N., Groves, D.I., 1984. Sulfur isotope composition and genesis of Archean gold mineralization, Australia and Zimbabwe. In: Foster, R.P. (Ed.), Gold'82. Balkema, Rotterdam, pp. 373–387.

Lang, D.Y., 1990. Geological characteristics and ore-forming conditions of the Wulashan gold deposit, Inner Mongolia. J. Inner Mong. Geol. 2, 30–40, in Chinese.

Li, S.X., Liu, X.S., Jin, W., Zhang, L.Q., 1990. Characteristics of auriferous ductile shear metamorphic zone, with central Nei Mongol as example. Selected Papers on the Geology of Gold Deposits, vol. 1. Geological Publishing House, Beijing, pp. 62–72, in Chinese.

Lin, E.W., Guo, Y.J., 1985. Lead isotope on gold fields in East Hebei, People's Republic of China. Changchun Coll. Geol. J. 42, 1–10, in Chinese with English abstract.

Meng, Q.C., 1986. A preliminary discussion on the fault-folding belt and marginal rift of ancient continent in the Yinshan area. J. Nonferrous Met. Geol. Inner Mong. 1, 1–7, in Chinese.

Miller, L.D., Goldfarb, R.J., Nie, F.-J., Hart, C.J.R., Miller, M.L., Yang, Y., Liu, Y., 1998. North China gold: a product of multiple orogens. Soc. Econ. Geol. Newsl. 33 (1), 6–12.

Mutschler, F.E., Griffin, M.E., Stevens, D.S., Shannon, S.S., 1985. Precious metal deposits related to alkaline rocks in the north American Cordillera: an interpretive review. Geol. Soc. S. Afr. Trans. 88, 355–377.

Nakai, S., Masuda, A., Shimizu, H., Lu, Q., 1989. La–Ba dating and Nd and Sr isotope studies on the Baiyun Obo rare earth element ore deposits, Inner Mongolia, China. Econ. Geol. 84, 2296–2299.

Nie, F.-J., 1993. Genesis of the Bieluwutu volcanogenic copper deposit, south-central Inner Mongolia, People's Republic of China. Int. Geol. Rev. 35, 805–842.

Nie, F.-J., 1998. Geology and origin of the Dongping alkalic-type gold deposit, northern Hebei province, People's Republic of China. Resour. Geol. 48, 139–158.

Nie, F.-J., Bjørlykke, A., 1994. Lead and sulfur isotope studies of the Wulashan quartz-K feldspar and quartz vein gold deposit, southwestern Inner Mongolia, People's Republic of China. Econ. Geol. 89, 1289–1305.

Nie, F.-J., Wu, C.Y., 1998. Gold deposits related to alkaline igneous rocks in north China craton, People's Republic of China. Global Tecton. Metallog. 6 (3 and 4), 159–171.

Nie, F.-J., Wu, C.-Y., Zhang, H.-X., 2000. Alkaline magmatism and gold metallogeny of the Baotou–Bayan Obo area, Inner Mongolia, China. Open File Rep.-Chin. Acad. Geol. Sci. (231), 1–56 (in Chinese).

Ohmoto, H., 1986. Stable isotope geochemistry of ore deposits. Rev. Mineral. 16, 491–560.

Ohmoto, H., Rye, R.O., 1979. Isotopes of sulfur and carbon. In: Barnes, H.D. (Ed.), Geochemistry of Hydrothermal Ore Deposits. Wiley, New York, pp. 509–567.

Peters, S.G., Golding, S.D., 1987. Relationship of gold-quartz mineralization to granodioritic phases and mylonites at Charters Tower goldfield, northeastern Queensland. The Geology, Structure, Mineralization and Economics of the Pacific Rim. Proceedings of Pacific Rim Congress. Australasian Institute of Mining and Metallurgy, Carlton Victoria, Australia, pp. 363–367.

Phillips, G.N., Groves, D.I., Neall, F.B., Donnelly, T.H., Lambert, I.B., 1986. Anomalous sulfur isotope compositions in the Golden Mile, Kalgoorlie. Econ. Geol. 81, 2008–2015.

Richards, J.P., 1995. Alkalic-type gold deposits: a review. In: Thompson, J.F.H. (Ed.), Magmas, Fluids and Ore Deposits. Mineral. Assoc. Canada, Short Course, vol. 23, pp. 267–400.

Richards, J.P., Kerrich, R., 1993. The Porgera gold mine, Papua New Guinea: magmatic-hydrothermal to epithermal evolution of an alkalic-type precious metal deposit. Econ. Geol. 88, 1017–1052.

Sengor, A.M.C., Natal'in, B.A., 1996. Paleotectonics of Asia: fragments of synthesis. In: Yin, A., Harrison, M. (Eds.), The Tectonic Evolution of Asia. Cambridge Univ. Press, London, pp. 486–640.

Shen, Q.H., Zhang, Y.F., Gao, J.F., Wang, P., 1990. Study on Archean metamorphic rocks in mid-southern Inner Mongolia of China. Chin. Acad. Geol. Sci., Inst. Geol. Bull. (21), 34–76, in Chinese with English Abstract.

Stacey, J.S., Kramers, J.D., 1975. Approximation of terrestrial lead

isotope evolution by a two-stage model. Earth Planet. Sci. Lett. 26, 207–221.

Taylor, B.E., 1987. Stable isotope geochemistry of ore-forming fluid. Mineralogical Association of Canada Short Course Handbook, vol. 13. Geological Survey of Canada, Ottawa, pp. 337–445.

Trumbull, R.G., Morteani, G., Li, Z., Bai, H., 1992. Gold metallogeny in the Sino-Korean Platform. Springer-Verlag, Berlin, 202 pp.

Wang, Q., Liu, X.Y., 1991. Pre-Jurassic tectonic evolution between Cathaysia and Angaraland in Inner Mongolia of China. In: Ishii, K., Liu, X.Y., Ichikawa, K., Huang, B.H. (Eds.), Pre-Jurassic Geology of Inner Mongolia, China. Matsaya Insatsu, Osaka, Japan, pp. 127–149.

Wang, H.Z., Mo, X.X., 1995. An outline of the tectonic evolution of China. Episodes 18, 6–16.

Wang, Y., Jiang, X.M., Wang, Z.K., 1990. Characteristics of lead and sulfur isotopes of the gold deposits in the Zhangjiakou–Xuanhua area, Hebei province, PRC. Contrib. Geol. Miner. Explor. 5, 66–75, in Chinese with English abstract.

Wang, J., Li, S.Q., Wang, B.L., Li, J.J., 1992. The Langshan-Bayan Obo Rift System. Beijing Univ. Publishing House, Beijing, pp. 1–132, in Chinese with English abstract.

Wu, S.F., 1993. Tectonic interpretation of Wulashan–Daqingshan area based on remote data. J. Gold Geosci. Technol. (1), 57–67, in Chinese.

Yuan, Z.X., Bai, G., Wu, C.Y., Zhang, Z.Q., Ye, X.J., 1992. Geological features and genesis of the Bayan Obo REE ore deposit, Inner Mongolia, China. Appl. Geochem. 7, 429–442.

Zartman, R.E., Haines, S.M., 1988. The plumbotectonic model for Pb isotope systematics among major terrestrial reservoirs—a case for bi-directional transport. Geochim. Cosmochim. Acta 52, 1327–1339.

Zhang, L.Q., 1989. Distribution and geologic features of gold deposits along the northern margin of the North China platform (within Inner Mongolian Autonomous Region). Geol. Soc. Inner Mongolia Bull. 11, 1–6, in Chinese.

Zhang, H.T., 1991. Granitoid magma series and gold metallogeny of the Baotou–Bayan Obo district, Inner Mongolia. PhD Thesis. Geol. Univ. China, Beijing, 126 pp., unpublished, in Chinese.

Zhang, H.T., So, C.S., Yun, S.T., 1999. Regional geologic setting and metallogenesis of central Inner Mongolia, China: guides for exploration of mesothermal gold deposits. Ore Geol. Rev. 14, 129–146.